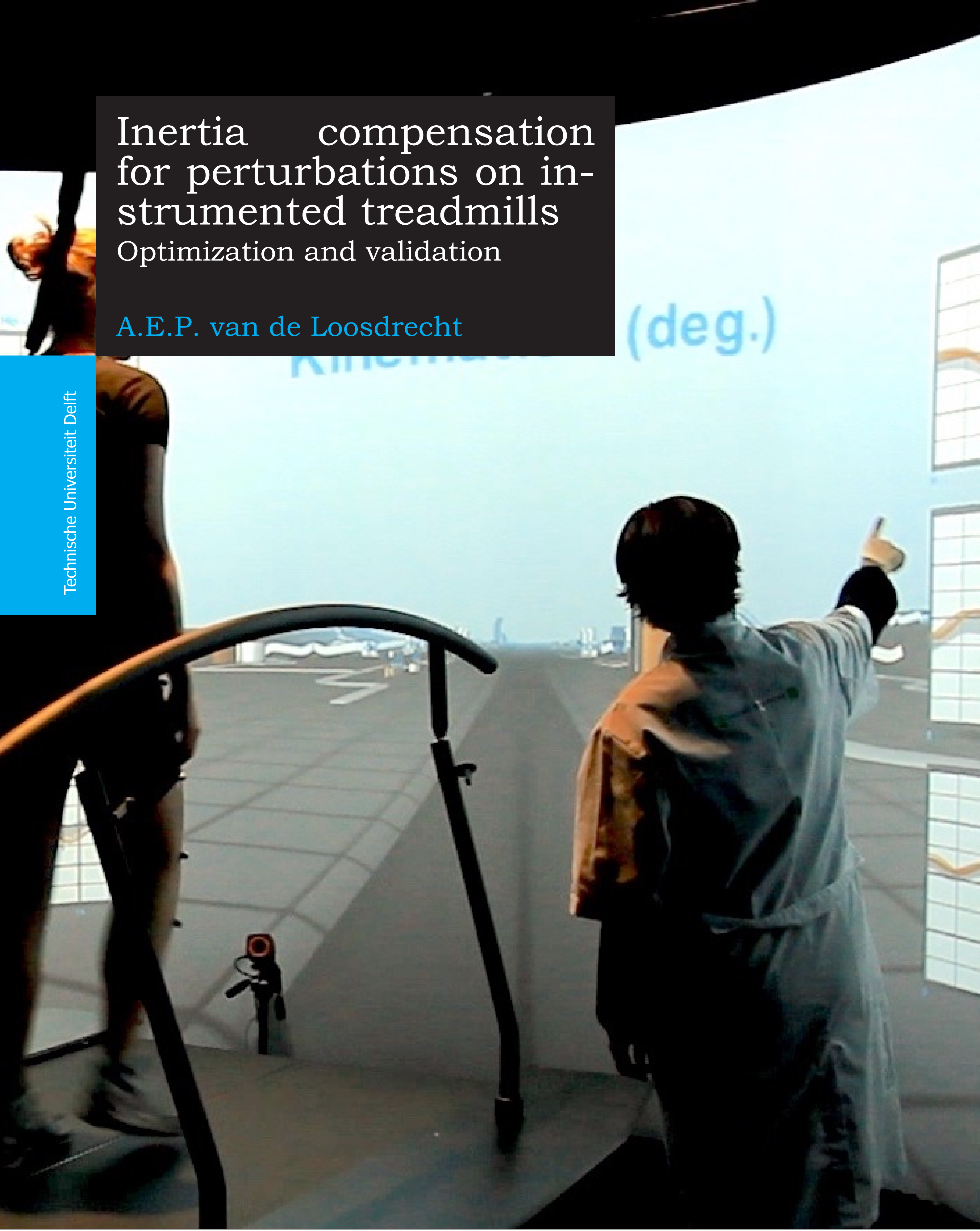

Inertia compensation for perturbations on instrumented treadmills

Optimization and validation

A.E.P. van de Loosdrecht

Technische Universiteit Delft

TU Delft Delft University of Technology

Challenge the future

Inertia compensation for perturbations on instrumented treadmills

Optimization and validation

by

A.E.P. van de Loosdrecht

to obtain the degree of

Master of Science
in Biomedical Engineering

at the Delft University of Technology,
to be presented on Thursday January 10, 2019 at 12:00 PM.

Student number:	4517687
Supervisors:	Prof. dr. Frans van der Helm & Phd. Selma Papegaaij

An electronic version of this thesis is available at http://repository.tudelft.nl/.

Preface

This thesis is the final result of my master in Biomedical Engineering at the TU Delft and of a collaboration between the TU Delft and Motekforce Link.

The main objective of my thesis was to optimize and validate an inertia compensation model that can be used during perturbations on instrumented treadmills. This thesis consists of a scientific paper that describes my entire research in a brief manner. More background information can be found in the first three appendices. Appendix D provides more detailed information about the methods that I used during this project. This information can be used for future students or researchers that want to continue with the data that has been obtained so far. The last few appendices contain extra results that were not shown in the paper. The informed consent form and participant information are also attached.

After having done my bachelor Biomedische Technologie in Groningen and the master Biomedical Engineering in Delft I have gained both clinical and engineering knowledge. The combination of which I find very interesting and has led me to this master thesis. After finishing most of the courses of the first year of the master it was clear to me that biomechatronics and especially musculoskeletal models fascinate me. Therefore, I went to prof. Frans van der Helm to discuss internship opportunities. From the start of my search of finding an internship, doing my literature study and setting me up with Motek he has helped me out. Despite his busy schedule he always managed to quickly solve problems that seemed very big to me. I would like to thank my supervisor prof. Frans van der Helm for his time and advice.

Also, I'd like to express my highest gratitude to Motekforce Link for allowing me to use their hardware, for all the support during the adversities that I encountered during my research and for the great time. I would especially like to thank Selma Papegaaij for the weekly meetings in which she helped me with many problems that allowed me to continue with the project. As I did not work with the GRAIL before, this had its ups and downs. I want to thank everyone from the clinical Applications Department for the support with all of small and sometimes bigger problems with both this software and hardware. From a development perspective, the developers helped me out a lot with the more technical questions and problems. I'd also like to express my gratitude to the participants of the experiment without whom the research would not have been possible.

Finally, I would like to thank my family and friends. My parents for being unconditionally helpful and supportive throughout my entire study. All my teammates and other people I enjoyed sailing with to take me out of my 'Matlab world' during the weekends which gave me a lot of energy and got me recharged time after time. My 'musketiers' for always being there for me and their always smart remarks. Jelle and Max for discussing all study related topics into great depth. And, of course all other friends, both from Delft and Groningen, for their support, and great company during coffee breaks.

This master thesis was uploaded to the TU Delft repository (`https://repository.tudelft.nl/`). All raw data from the experiments, the Matlab files and D-Flow applications are submitted to the depository of the department of BioMechanical Engineering and are available on request.

Arianne van de Loosdrecht
Delft, 31st of December 2018

Contents

Preface iii

1 Scientific paper 1
1.1 Introduction 2
1.2 Methods 3
1.3 Results 6
1.4 Discussion 9

A Dynamic validation 15
A.1 Force measurements 15
A.2 Error in dynamic force plate measurements 16
A.3 Accuracy 16
A.4 Linearity 16
A.5 Delay 17
A.6 Static calibration 17

B Human Body Model 19
B.1 Numerical methods 19
B.1.1 Inverse kinematics 20
B.1.2 Inverse dynamics 20
B.1.3 Muscle forces 20
B.2 Kinetic residuals 20

C Inertia compensation model 23
C.1 Dynamics of the inertia compensation method 23

D Methods 27
D.1 Dynamic validation 27
D.1.1 Data acquisition 27
D.1.2 Static calibration 28
D.1.3 Accuracy 28
D.1.4 Linearity 29
D.1.5 Delay 29
D.2 Data analysis 29
D.3 Optimal calibration trial 30
D.3.1 Equipment 30
D.3.2 Interaction between models 30
D.3.3 Pitch and Sway 30
D.3.4 Belt accelerations 31
D.3.5 Signals 31
D.4 Data analysis 32
D.5 Effect of inertia compensation on a musculoskeletal model 32
D.5.1 Equipment 32
D.5.2 Experimental design 32
D.5.3 D-Flow application 32
D.5.4 Subjects 33
D.5.5 Data processing 33
D.5.6 Data analysis 33
D.5.7 Statistical analysis 34

E Signals optimal calibration trial **35**
E.1 Calibration trials . . . 35
E.2 Validation trials. . . . 36
E.3 Calibration trials pitch and sway . . . 37
E.4 Calibration trials belt acceleration. . . . 38

F Experiment results **39**
F.1 Dynamic validation results . . . 40
F.2 Optimal calibration trial results . . . 41
F.2.1 Interaction between models. . . . 41
F.2.2 Plots for all validation trials. . . . 41
F.2.3 Best calibration trial pitch and sway . . . 43
F.2.4 Speed and duration pitch and sway. . . . 43
F.3 Evaluation of IC model results . . . 44
F.3.1 Estimated marginal means for all measures . . . 44
F.3.2 Raw data of the kinetic residuals of one subject . . . 45

G Consent Form **53**

H Participant Information Sheet **55**

Bibliography **59**

1

Scientific paper

Optimization and validation of an inertia compensation model for instrumented treadmills

Arianne E.P. van de Loosdrecht[1], Selma Papegaaij[2], Frans C.T. van der Helm[3]

Abstract— **Instrumented treadmills and perturbations of the treadmill are commonly used for gait analysis and can provide real time biomechanical information and feedback of gait patterns and abnormalities. Force plates in the treadmill are combined with motion capture data and fed into a musculoskeletal model. High accuracy of the force plates is needed to give reliable feedback for gait analysis. The accuracy still needs to be tested under dynamic conditions, with the belt running. Also, inertial and gravitational forces are measured during perturbations as a result of the rotation and translation of the platform in which the force plates are positioned. This results in an error in the forces and moments as measured by the force plates, which is added up to the forces exerted by a subject. Inertia compensation models have been developed and showed promising results but have not been validated extensively. This study aimed to optimize and validate an inertia compensation model for perturbations on instrumented treadmills and validate the force measurements under dynamic conditions. It was shown that the treadmill can accurately measure the center of pressure (error = 1-6 mm), forces (error = 1-7 N) and moments (error = 0.5-4 Nm). A new calibration trial was found with higher sway accelerations which improved the inertia compensation model and left residuals forces and moments below 2 N(m). Moreover, it showed that using this inertia compensation model for pitch and sway trials led to a reduction of the kinetic residuals of up to 96% and values close to baseline measurements.**

Keywords: **Gait analysis, musculoskeletal model, inertia compensation, biomechanics, instrumented treadmill, perturbations**

I. INTRODUCTION

Clinical gait analysis can be used to improve assessment and treatment of people with walking impairments that can be due to either neurological, orthopedic or neuromuscular deficits. Another application of gait analysis is in sports, where it can help to improve performance or prevent injuries of the athletes by providing information on the biomechanics [1].

Instrumented treadmills are nowadays commonly used for gait analysis [2]. The instrumented treadmills can provide real time biomechanical information and feedback of gait patterns and abnormalities while a subject is walking on a motorized treadmill. An integrated force plate (FP) can measure ground reaction forces and the center of pressure (COP). This information can be combined with a motion capture system which together give information on temporal parameters, kinematics, kinetics and muscle forces. All of this may assist to improve identification of neuromusculoskeletal impairments and their effect on walking and balance. This information can be calculated using the instrumented treadmill data and a musculoskeletal model. Outputs of the musculoskeletal model can involve joint angles, joint forces and moments, joint power and muscle forces. Many different musculoskeletal models exist with a wide range of complexity, many different calculations and various assumptions [3][4].

An increasingly used feature of the instrumented treadmills is the possibility to perturb gait and posture of subjects. Perturbations can train balance and challenge subjects even more than during normal gait analysis. Suddenly swaying the entire platform laterally or rapidly accelerating or decelerating the belt can induce perturbations. Both methods of are used in research as well as in clinical settings [5][6]. Another way of perturbing is rapidly pitching the treadmill. This is less common practice, however, as the magnitude of the perturbation is dependent on the position of the subject on the belt. Nevertheless, pitching is a widely used method to simulate up- and downhill walking.

The instrumented treadmills and corresponding musculoskeletal models are widely used. Despite this wide use, earlier research shows that biomechanical information as calculated by a musculoskeletal model is still prone to errors. This is mainly due to inaccurate measurement of ground reaction forces and kinematic data [7][8]. It is, however, of great importance to obtain reliable results in order for clinicians as well as researchers to use the data retrieved by the treadmills. This results in a high need for quality checks of the instrumented treadmills and validation and verification of the musculoskeletal models [9][10].

Part of the error in the musculoskeletal model output can be due to inaccuracy of motion capture systems. These have, however, been tested extensively and have shown results with only 2mm errors during dynamic conditions [11]. Another error source can be the inaccuracy of the force plates. Larger errors can be expected in the FPs incorporated in the instrumented treadmills compared to overground FPs due to movements and a limited weight of the force plates. A delay between the motion capture data and force plate data can also result in an error in the output of a musculoskeletal model.

Static evaluations of the FPs are commonly done to prevent inaccuracies. Extensive static evaluation involves analysis of accuracy, drift, noise, linearity, hysteresis and

---

[1] A.E.P. van de Loosdrecht is with the Department of Biomechanical Engineering, Faculty 3mE; Delft University of technology, Mekelweg 2, 2628 CD Delft, The Netherlands, and with Motekforce Link, Hogehilweg 18C, 1101 CD Amsterdam, The Netherlands.

[2] S. Papegaaij is with Motekforce Link, Hogehilweg 18C, 1101 CD Amsterdam, The Netherlands.

[3] F.C.T. van der Helm is with the Department of Biomechanical Engineering, Faculty 3mE; Delft University of technology, Mekelweg 2, 2628 CD Delft, The Netherlands.

cross-talk [12]. A static validation has also been done for Motekforce Link's R-Mill as described in an earlier paper [13]. Dynamic evaluation of the force plates, with the belts running, might give even more insights on the measurements. Testing in dynamic circumstances seems necessary to be able to ensure the quality of the treadmill as the force plates in the treadmill are often used under these conditions. However, the dynamic evaluation is less common practice and mostly done less extensive [14]. It is therefore still unclear what the quality of the force plates is under dynamic circumstances.

The introduction of perturbations also brings new challenges for force measurement. Earlier research shows that the measurement of forces during perturbations is not accurate enough [15][16]. Inertial and gravitational forces are measured during perturbations as a result of the rotation and translation of the platform in which the force plates are positioned. However, the only forces and moments of interest for further calculations are the forces and moments exerted by a subject. The extra inertial and gravitational forces therefore result in an error in the forces as measured by the force plate. Subsequently, all of the measured forces, including the corresponding error, are used in the calculations of the musculoskeletal model. In the end this results in wrongly calculated joint moments and forces of the subject.

Two innovative ways were found to compensate for the forces that are not exerted by subjects, both by using inertia compensation (IC) models. The IC models are especially applicable for instrumented treadmills and showed promising results [15][16]. The first IC model compensates for the artifacts due to sway and pitch movements of the instrumented treadmill using accelerometers. The second model compensates for the pitch moment that is created during belt accelerations and decelerations. The quick belt accelerations result in a torque of the motor which in turn results in a pitch moment. This IC model is based on the belt speed of the treadmill. The IC models are calibrated using trials with perturbations. The IC models are not perfect so far and a small error still remains. It is, nonetheless, thought that other calibration trials can result in better IC models. Up and until now no research has been done on this part.

An extensive validation of these inertia compensation models still lacks as well. Only a technical validation of the IC models has been done so far. The technical validation only showed what the effect of the IC model is on the measured forces. These papers on IC models show that forces and moments were lowered to an acceptable level to perform a useful inverse dynamic gait analysis on. Nonetheless, good verification and validation requires testing of the IC models in the real world to be able to draw conclusions on the reliability of the model for researchers and clinicians [9]. The effects of the IC model on the outcomes of the musculoskeletal model with a subject on the treadmill have not been researched yet.

The main goal of this study was therefore to optimize and validate an inertia compensation method for perturbations on instrumented treadmills. In order to do so a few subgoals were set up:

A) Dynamically validate the force plates of an instrumented treadmill.
B) Optimize the calibration trial on which the inertia compensation model is based.
C) Evaluate the inertia compensation model in a real world situation including subjects.

Here we have dynamically validated the force plates of the instrumented treadmill using motion capture data and calibrated weights. Moreover, an optimization of the calibration trial on which the inertia compensation model is based was done by looking at the remaining error for several different calibration trials. Lastly, the IC model was evaluated in an experiment in which the outcomes of the musculoskeletal were evaluated after testing with a subject walking on the instrumented treadmill. For this, the hypothesis is that the error of the musculoskeletal model is lower when using the inertia compensation model while walking with perturbations than without the IC model.

II. METHODS

A. Exp. 1: Dynamic validation of the force plates

The goal of the first experiment is to validate the force plates of an instrumented treadmill. The accuracy of force measurement and COP is validated. The linearity of force measurement is measured as well. Finally, the delay between motion capture data and force plate data is checked.

1) Equipment: For this entire study a 2-DOF instrumented treadmill with a split belt instrumented treadmill was used (GRAIL system with a R-mill, Motekforce Link, Amsterdam). The system was equipped with actuators capable of translation in the mediolateral direction (sway) and rotation for sagittal pitch. A Vicon motion capture system with ten infrared cameras was used. All data were obtained from Vicon Nexus 2.7. This included the accelerometer data (1000Hz), the force plate data (1000Hz) and the belt speed (200Hz) which was obtained by streaming the belt speed to Vicon using D-Flow software (Motekforce Link, Amsterdam).

2) Experimental design: The accuracy of the COP and force measurement was validated with the help of calibrated weights with a marker. Validation was done with the forces calculated from the calibrated weight and accelerations of the marker on top of the weight.

Several different conditions were used to test the force plates of the treadmill. Three different speeds were measured (0.3m/s, 0.7 m/s, and 1.0m/s) and four different weights were used (13.44kg, 22.56kg, 36.00kg, and 45.08kg). A distinction in speed profile was made between constant treadmill speed and acceleration. An experimental set-up was used with weights of 4.5kg on a rod with a marker on it. The weights were moved back and forth three times for each trial by moving the treadmill belt. Six different starting positions in mediolateral direction were chosen, three for each belt.

The first measurements showed that some low frequency vibration was present in the COP data from the FP in the z-direction. Noise amplitudes were seen of up to three centimeters. One of the reasons for this could be a vibration of the weights relative to the metal pole. In this set-up there is some space between the weights and the pole which could cause some movement and thus changes in COP. To exclude this possibility, an extra experiment was done in which one marker was placed on the pole and one on the weight during a trial. No difference in distance between those two markers was found, which indicates no vibrations on this part. Another reason for the vibration could be due to some movement around the pitch axis of the treadmill due to a somewhat flexible basis of the platform and the pitch motion mechanism. It has been shown before that using two metal supports underneath the treadmill can prevent this [17]. Therefore in the second set-up, two metal supports, one on the left front and one on the rear right, were used to prevent this motion. This set-up is the same as Motekforce Link advises to use in gait analysis.

3) Data analysis: A static calibration was done before the analysis to prevent misalignment of the motion capture and force plate coordinate systems as proposed by Goldberg et al. (2009) [18]. Accuracy of the force plates was calculated with the root mean square error (RMSE):

$$RMSE = \sqrt{\frac{\sum(F_{FP} - F_{marker+weight})^2}{n}} \tag{1}$$

Where F_{FP} are the force plate data, $F_{marker+weight}$ are the forces calculated from the accelerations of the markers and the known calibrated weights and n is the sample size. Accuracy of the COP of the FP was then calculated in two different ways. First of all by taking the differences between the marker data and the COP measured by the FP, as most common in literature. As this does not take into account uncertainty in marker data, a second method to calculate the error was performed using Total Linear Least Squares (TLLS)[19]. These calculations were done in Matlab 2016b with the singular value deposition method and a Matlab Toolbox (*Total least squares method*) was used as a basis [20].

Another part of the validation was the validation of the linearity of the force measurement. To calculate the linearity, a linear least squares polynomial was fit through the known loads versus the measured loads. The differences between the measured forces and this fit would then show linearity. To exclude outliers, three times the standard deviation of these differences was taken as non-linearity measure. Furthermore, a second order linear least squares polynomial was fit through the measured loads data. The fit was then evaluated by calculating R^2 for both the first and second order polynomial.

Delay between the motion capture data and force plate data was tested as well. For this, it is important to know the time difference between the first moment a force is applied and the first moment a force is measured. Both belts were hit with a hammer with a marker for fifteen times. The first moment at which the marker was at it lowest vertical position was taken as the first instance on which the hammer hit the force plate. The moment at which the measured force first exceeded five times the standard deviation above or below the baseline was used as the moment on which force was measured.

4) Statistical analysis: Differences between groups (e.g. different speeds, different anterior/posterior (AP) positions et cetera) were studied using a three way analysis of variance in Matlab (ANOVAN) ($\alpha = 0.05$) after a Boxcox transformation was done to obtain a normal distribution. A Bonferroni correction was used to correct for multiple comparisons. All data were low-pass filtered with a cut-off frequency of 20Hz with a second order Butterworth filter and using zero-phase digital filtering. For the constant speed trials, high accelerations were present just before and after changing direction of movement. Because of this only the data from the middlemost 50% of the treadmill of these trials were used.

B. Exp. 2: Optimization of calibration trial

In the second experiment different inertia compensation models were made based on several different calibration trials. The IC models were then checked with validation trials. This was done for an IC model for pitch and sway perturbations and for an IC model for belt perturbations.

1) Equipment: The same equipment was used as in experiment 1 with the addition of two triaxial accelerometers (4030 2G range, Measurement Specialties). Figure 1 shows the set up with accelerometers.

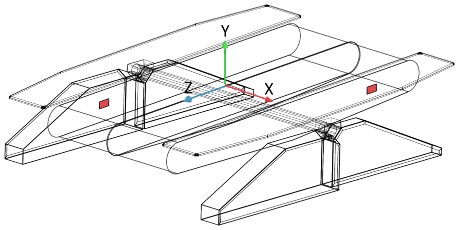

Fig. 1. Treadmill set up with the accelerometers in red and the coordinate system x-y-z [16].

2) Experimental design: The inertia compensation model was divided into a part with pitch and sway perturbations [16] and a part with belt perturbations [15]. Both methods used in this study were similar to the methods in these papers. No interaction between these two models was found.

For pitch and sway IC, a calibration trial consisted of perturbations of an empty treadmill. The forces measured by the force plate and the accelerations measured by the accelerometers formed the basis for an inertia compensation model. This was done in Matlab using the backslash operator:

$$C = A_{caltrial} \backslash F_{caltrial} \tag{2}$$

Where A is the matrix with measured accelerometer data, F is the matrix with the forces as measured by the force plate and C is the inertia compensation matrix, similar to the mass matrix. All training trials were run for a duration of 60 and 300 seconds and with a speed of 0 (with the motor running) and 3 m/s.

This lead to an IC matrix for each calibration trial. A second type of trial, a validation trial, was then used to test every IC matrix on. Four different validation trials were used. For each validation trial a person was walking on the right belt. The forces of the empty, left belt were used for analysis.

A) **Sway perturbations** A subject walking on the right belt (speed 1.3m/s) with perturbations similar to normal use (speed = 0.31m/s and amplitude = ±0.05m).
B) **Pitching** A subject walking on the right belt (speed 1.3m/s) with a sinusoidal movement of pitching (-10° to 10° with a wavelength of 30 seconds).
C) **Running** A subject running on the right belt (speed 2.5m/s).
D) **Boarding** A subject on the boarding of the treadmill to simulate movements that a subject exerts on the treadmill when walking on it.

During these validation trials, force measurements were captured and forces were predicted using the IC matrix and accelerometer data with the following equation:

$$\hat{F} = A_{valtrial} * C \tag{3}$$

Where A is the matrix with measured accelerometer data from the validation trial, C the inertia compensation matrix obtained with the calibration trial and F the estimated forces.

For the belt accelerations IC, the methods were similar to the paper of Hnat (2014) [15]. A linear second-order discrete time model was used to predict the forces based on the belt speed. The belt speed was derived with the use of a central difference formula using the gradient function in Matlab. In Matlab, fmincon was used to minimize the sum of the squared error between the estimated forces and measured forces. Using the model, the forces and moments were calculated for following trials. Again, the difference between the predicted forces and measured forces was seen as the error. One validation trial was used to test the model on. The validation trial included a part with random accelerations and a part with perturbations similar to normal use. All calibration trials were run for 60 and 300 seconds and with a base speed of 1 and 2 m/s.

3) Data analysis: For both compensation methods, the difference between the predicted forces and measured forces was seen as the error. A smaller error indicated better inertia compensation and thus a better calibration trial. This was calculated as following:

$$RMSE = \sqrt{\frac{\sum(\hat{F} - F_{valtrial})^2}{n}} \tag{4}$$

Where n is the number of samples, $\hat{F}$ the forces as calculated by Equation 3 and $F_{valtrial}$ the measured forces in the validation trial.

The belt speed was obtained at 200Hz, whereas the forces were obtained at 1000Hz. However, the output of the belt speed was given in 1000Hz. The steps of the 1000Hz signal were not discrete due to some noise and were thus filtered with a second order Butterworth filter. A cubic spline smoothing method (csaps Matlab) was used to obtain the optimal cut-off frequency for this filter: $wo = (p{*}T)^{(}-0.5/M)$ with wo the cutoff frequency, p the smoothing parameter, T the sampling interval, and 2M the order of the spline [21]. This resulted in a 10Hz cut-off frequency which was used for both the belt speed and the pitching moment. With a typical cut-off frequency of 6Hz for gait analysis, 10 Hz seemed appropriate for a little higher frequency movements like during perturbations.

4) Statistical analysis: A ranking was made in order to be able to choose the best calibration trial. This ranking was based on the percentage of root mean square error (RMSE) reduction of the forces. All calibration trials were ranked for each combination of the four validation trials and six forces and moments. An overall ranking was made for each calibration trial using the average of 24 rankings. For each combination of a validation trial and a force, the best calibration trial was chosen, all based on percentage of RMSE reduction. The calibration trial that ended up most in both the ranking and the best trial table was chosen as the best calibration trial. The two different speeds and two different durations were compared as well. This was done using the best calibration trial with the help of a n-way analysis of variance in Matlab (ANOVAN). A Bonferroni correction was used to compensate for multiple comparisons.

C. Exp. 3: Evaluation of the inertia compensation model

In experiment 3 the effect of the inertia compensation model on the outcomes of the musculoskeletal model was evaluated. This was done by looking at the kinetic residuals of the musculoskeletal model while subjects were perturbed.

1) Equipment: The same set up as for experiment 1 and 2 was used. This time the data were processed with D-Flow software (Motekforce Link). A safety harness for the subjects was added and attached to the ceiling. Subjects were provided with 46 markers as specified for the musculoskeletal model (Human Body Model, Motekforce Link) [3].

2) Experimental design: A total of 10 young, healthy adults participated in the experiment. Data of only 9 subjects (mean age 26 (± 3.8)years) were used due to poor marker data of one of the subjects. All participants were between 18 and 35 years old without any neurological or orthopedic conditions that could influence balance or walking. Six males and three females participated (mean length 1.78m (± 0.13m), mean weight 74.6 kg (± 11.45kg)) and were all wearing their own sneakers. All participants gave their informed consent. The study was approved by the Human Research Ethics Committee of the TU Delft.

Only the pitch and sway inertia compensation method was evaluated as the belt perturbation method was not yet implemented in the D-Flow software. The experiment consisted of one familiarization trial and three trials with different conditions. The familiarization trial included six minutes of walking on the treadmill at an average walking speed for young healthy adults (1.3m/s) [22]. Subjects were instructed to walk as normal as possible. Each trial started with a subject standing still with their arms spread (Tpose).

- **Baseline measurement.** Two minutes of normal walking without any perturbations.
- **Sway perturbations.** About twelve minutes of walking with 20 ipsilateral sway perturbations at initial contact. During a perturbation the entire platform was moved laterally for 5cm with a speed of 0.30m/s. The platform was slowly returned to base after seven seconds. Time between perturbations was chosen randomly, the same for all subjects however, between 10 and 60 seconds. Perturbations were randomly divided over the left and right foot.
- **Pitching.** Two minutes of up and downhill walking (a sinusoidal signal from -10° to 10° of pitch with a wavelength of 30s).

The inertia compensation model was trained on the best trial obtained from the second experiment (a random signal with a square wave of sway of 300 seconds). The inertia compensation matrix from the second experiment was used to correct the forces before they were fed into the Human Body Model [3].

3) Data analysis: All data were processed using D-Flow 3.32. A hundred steps were used from the baseline and pitch trials. For the sway trial only the data during a perturbation was used. The weight of the subject was obtained by force plate data of the first 100 frames of a trial with a person in Tpose.

The measures used were the kinetic residuals of the Human Body Model [3]. The Human Body Model combines the motion capture and force plate data for inverse kinematics and inverse dynamics. The forces that cannot be prescribed to any joint are prescribed to the pelvis and are called the residual forces and moments. The Human Body Model uses six different kinetic residuals which are all described relative to the global reference frame: Force in the x-, y- and z-direction and the moments around the x-, y- and z-axis. In this setting the x-axis points forward, the y-axis to the right and the z-axis upwards. The global coordinate system does not exactly align with the kinematical coordinate system of the pelvis but will most often be nearly the same. The kinetic residuals can be seen as the experimental and modeling error and are therefore a good measure of the musculoskeletal model accuracy.

4) Statistical analysis: The root mean square (RMS) of all six kinetic residuals was calculated for each condition for each subject in Matlab. The entire statistical analysis was performed in SPSS 25.0. A 2 (IC) x 3 (conditions) repeated measures two-way ANOVA ($\alpha = 0.05$) was performed. A paired samples t-test was performed for comparison for each condition with and without IC. Also, sway with IC and pitch with IC were compared to baseline without IC. A Bonferroni correction was used for these five multiple comparisons. A non-parametric test was done besides the parametric test because the subject data was non-normally distributed. The Friedmans test was used as a non-parametric equivalent for the repeated measures two-way ANOVA. A Wilcoxon signed rank test was used in the same way as the paired samples t-test for the parametric method. The same Bonferroni correction was used for the non-parametric test. The Greenhouse-Geisser correction was used if the assumption of sphericity was violated. The influence of length and weight of the subjects was evaluated by adding those as covariates in SPSS. The power was calculated with SPSS.

III. RESULTS

A. Exp. 1: Dynamic validation of force plates

1) General RMSE: By using the metal supports underneath the treadmill, the standard deviation of the noise reduced from 5cm to 3.5cm. The results of the calculations with the error as the difference between marker data and force plate data and the error calculated by TLLS are both shown in the first part of Table I. All variables are shown for the measurements with and without metal support. All the results were obtained with TLLS and metal supports.

2) Differences between parameters: The RMSEs for different speeds, starting positions, AP positions and different weights per variable can be seen in Table III-A.2. All parameters are significantly different from the other groups except for the AP positions. For the AP positions, only the back of the belt differed significantly from the front and middle. Figure 2 shows the results COP in the z-direction for different weights and speeds.

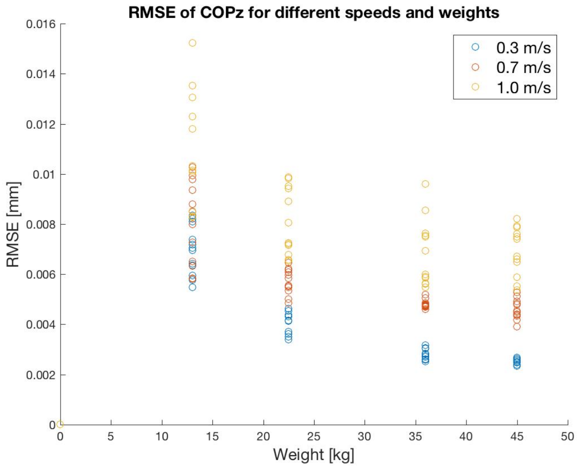

Fig. 2. RMSE of one trial for different anterior-posterior positions (AP) and speeds. All speeds differ significantly. The back of the belt differs significantly from the front and middle. The front and middle do not differ significantly from each other.

3) Static calibration: The static calibration was used to find the optimal rotation angle and offset to compensate for the misalignment between marker and force plate coordinate systems. This resulted in a rotation angle of 0.19°, an offset in the x-direction of 1.5mm and an offset of -1.8mm in the z-direction. These results were then used for all dynamic validation data to ensure coordinate system alignment.

4) Linearity: The linearity of the measured loads as defined earlier shows that with these data there is a non-linearity of 6.3N. With a full scale output of 510N this equals 1.3%. A second order linear least squares polynomial

TABLE I

ROOT MEAN SQUARE ERRORS FOR DIFFERENT CONDITIONS (SPEED, STARTING POSITIONS (STARTPOS), ANTERIOR POSITIONS (AP) AND WEIGHTS) AND FOR THE COP, FORCES (F) AND MOMENTS (M) IN ALL DIRECTIONS. THE FIRST PART SHOWS THE DIFFERENCES BETWEEN MEASUREMENTS WITH AND WITHOUT METAL SUPPORTS (SUPPORT - NO SUPPORT) AND BETWEEN THE DIFFERENT USED METHODS (NORMAL ERROR AND TLLS). THE START POSITION DISTANCES ARE MEASURED FROM THE LEFT PART OF THE BELT.

	COPx (mm)	**COPy (mm)**	**COPz (mm)**	**Fx (N)**	**Fy (N)**	**Fz (N)**	**Mx (Nm)**	**My (Nm)**	**Mz (Nm)**
Normal error - support	4.3	-	1.2	4.3	14.4	10.5	8.9	4.4	4.0
Normal error - no support	9.9	-	2.1	3.9	14.2	10.7	9.7	4.2	5.0
TLLS - support	0.9	-	5.4	1.0	1.8	7.4	3.6	2.8	0.6
TLLS - no support	1.1	-	13.2	1.0	2.1	7.7	3.8	2.9	0.6
speed = 0.3m/s	0.7	-	4.4	0.7	1.0	4.4	3.5	1.9	0.4
speed = 0.7m/s	0.9	-	6.0	1.3	1.9	7.3	2.6	3.0	0.6
speed = 1.0m/s	1.0	-	7.9	1.8	2.9	11.4	2.9	3.8	0.8
startpos = 0.15m	0.8	-	0.6	1.2	1.7	6.7	2.5	2.6	0.
startpos = 0.25m	0.8	-	0.6	1.1	1.7	7.0	4.2	2.6	0.6
startpos = 0.35m	0.8	-	0.6	1.1	1.7	6.7	2.5	2.6	0.6
AP = -0.55m	1.4	-	9.2	1.2	3.5	4.6	2.6	2.5	1.2
AP = -0.20m	1.2	-	6.2	0.9	3.0	4.4	1.5	1.6	1.0
AP = 0.19m	1.2	-	6.7	2.7	3.0	4.3	1.9	2.0	1.0
weight = 13.44kg	1.1	-	8.0	0.8	1.0	2.5	1.4	1.2	0.3
weight = 22.56kg	0.8	-	5.3	0.9	1.3	4.2	1.9	1.8	0.4
weight = 36.00kg	0.6	-	4.2	1.2	1.8	7.5	3.8	3.0	0.6
weight = 45.08kg	0.6	-	4.0	1.5	2.4	10.3	4.5	3.6	0.8

fit resulted in $R^2 = 0.99$ both for the first order fit and the second order fit.

5) Delay: The average delay between the marker data and the force plate data for the left and right belt were 0.004s and 0.002s respectively, with the force plate being later. The sampling frequency of the marker data was 100Hz whereas that of the force plate data was 1000Hz. The final result is therefore smaller than a frame of the motion capture system. No difference could be found in delay between the different positions on the belt.

B. Exp. 2: Optimization of calibration trial

1) Pitch and sway: In the ranking of RMSE reduction for each calibration trial the calibration trial with 300 seconds of random signal and with square waves of sway in it and a speed of 3m/s turned out to be the best. The calibration trial with 300ms of random signal and gaps in it and a speed of 3m/s ended up on a second place. This was followed by the 60 second trial with all of the variations in it and a speed of 3m/s.

The forces and moments during the pitching validation trial can be seen in Figure 3. The inertial artifacts as measured by the treadmill can be seen (measured). The forces as predicted with the help of the accelerometers based on the square wave of sway calibration trial (estimated) are compared to this. The difference between these two is the error (residual) which is still left after inertia compensation.

All the RMS results for the calibration trial with a square wave of sway in it can be seen in Table II. RMS raw is calculated from the measured data during the validation trials without inertia compensation. The RMS compensated is the data after the predicted inertial artifacts are subtracted. The RMS reduction is the percentage of RMS that is reduced between these two.

It can be seen that the validation trial with pitching gave the biggest inertial and gravitational artifacts without compensation. After inertia compensation, all of the forces and moments are reduced to less than 1 N or 1 Nm except for Fy which is still 2.3 N. For the running validation trial, the human ground reaction forces are relatively big. With a person applying a force to the boarding, inertial artifacts occur in several directions. The lowest RMS reduction for this trial is 85%.

TABLE II

ROOT MEAN SQUARE (RMS) RESULTS PER VALIDATION TRIAL FOR THE CALIBRATION TRIAL WITH A SQUARE WAVE OF SWAY IN IT. THE TABLE SHOWS THE RMS OF THE MEASURED FORCES (RMS RAW) AS WELL AS THE RMS OF THE FORCES AFTER COMPENSATION (RMS COMP). THE PERCENTAGE DIFFERENCE BETWEEN IS SHOWN AS THE RMS REDUCTION.

Validation trial	**Variable**	**RMS raw**	**RMS comp**	**RMS reduction (%)**
Pitching	*Fx (N)*	1.3	0.4	67
	Fy (N)	18.2	2.3	87
	Fz (N)	164.4	0.7	99
	Mx (Nm)	28.3	0.8	97
	My (Nm)	56.4	0.6	99
	Mz (Nm)	5.4	0.8	85
Running	*Fx (N)*	1.9	0.7	60
	Fy (N)	7.2	2.8	61
	Fz (N)	3.9	1.9	52
	Mx (Nm)	22.2	1.8	92
	My (Nm)	2.3	1.5	36
	Mz (Nm)	2.8	1.1	59
Sway	*Fx (N)*	60.7	1.1	98
	Fy (N)	3.9	2.1	46
	Fz (N)	3.8	1.6	57
	Mx (Nm)	11.0	1.3	88
	My (Nm)	7.7	1.3	83
	Mz (Nm)	7.2	0.8	89
Boarding	*Fx (N)*	18.8	1.0	95
	Fy (N)	12.8	2.0	85
	Fz (N)	61.5	1.8	97
	Mx (Nm)	38.3	2.0	95
	My (Nm)	21.3	1.1	95
	Mz (Nm)	5.1	0.7	86

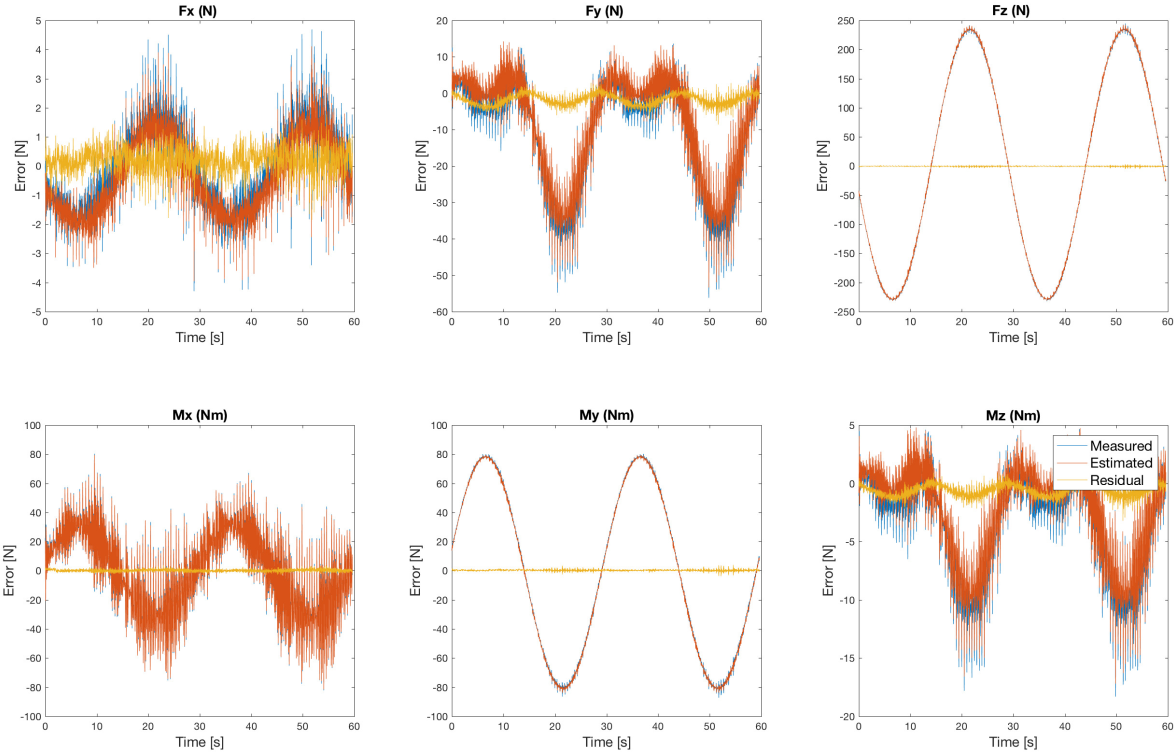

Fig. 3. The six different forces and moments are shown during the pitching validation trial. The estimated forces (orange) are subtracted from the measured forces (blue). The residual forces (yellow) are the differences between those two. The compensation matrix was based on the calibration trial with the square wave of sway in it. It can be seen that the residual force is only a few newtons or newton metres. Please note the different scales on the y-axes.

2) Belt perturbations: The residual error for all belt acceleration calibration trials was between 3 and 5 Nm and the RMS reduction between 80 and 83 per cent. The calibration trial with a random signal for 60 seconds plus perturbations ended up best in the ranking ($R^2 = 0.97$, RMS raw = $21.6Nm$, RMS compensated = $3.7Nm$, RMS reduction = 83%). The same trial with a duration of 300 seconds ended up second and the trial with a random signal and a square wave of sway ended up third. The measured pitch moment, estimated pitch moment and acceleration for the best calibration trial during part of the pitch validation trial can be seen in Figure 4, which is representative for the other three validation trials.

In first instance a validation trial was used similar to the ones for pitch and sway. A person walked on one belt and the forces from the other, empty belt were used. It was seen, however, that when using this, the RMS reduction of the inertia compensation was only around 7%. Using a calibration trial similar to the validation trial, so with a subject on the belt as well, showed far better results. It seems like a subject initiates a pitching moment for which the belt acceleration IC model cannot compensate as can be seen in Figure 5. Therefore, a validation trial without a subject on the treadmill was used. This does mean that compensation for a person on the treadmill is still needed.

3) Speed and duration: Two different speeds and durations were examined to obtain the best calibration trial for both pitch and sway and for belt accelerations. A significant difference between speeds and between durations was found for every force and moment in the pitch and sway trials. A belt speed of 3 m/s was best for four out of six variables (for Fx, Fz, Mx and for My). A duration of 60 s was best for three out of six variables (Fy, Mx and Mz). No significant differences could be found in the belt acceleration

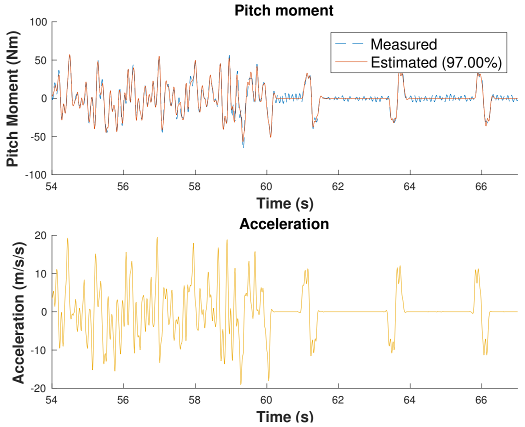

Fig. 4. The measured pitch moment, estimated pitch moment and acceleration during part of the validation trial. It can be seen that 97% of the pitch moment can be compensated by the model. The model was based on a calibration trial with 60 seconds of random accelerations and a part with perturbations similar to normal use.

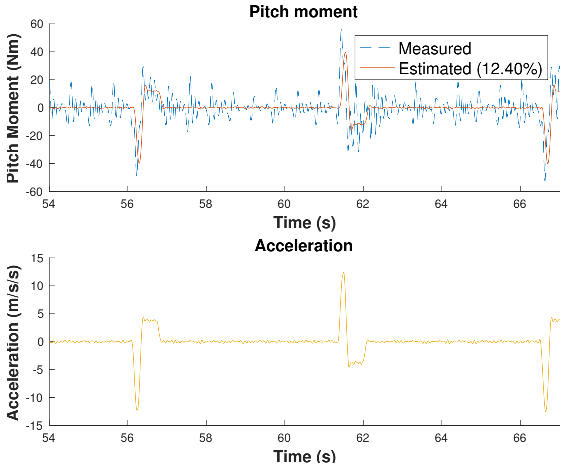

Fig. 5. The measured pitch moment, estimated pitch moment and acceleration during part of a validation trial with a subject on the opposite belt. It can be seen that the noise of the measured forces (blue) is not simulated (orange) entirely.

trials between different speeds (1 and 2 m/s) and different durations (60 and 300 s).

C. Exp. 3: Evaluation of inertia compensation model

Figure 6 and 7 show the kinetic residuals during a gait cycle for pitch and sway, respectively. The results for the baseline measurements with and without inertia compensation are compared with the results for the perturbation trials with and without inertia compensation. It can be seen that for the pitching trials mainly the force in the x-direction and the moment in the y-direction are improved. For the sway trials only the data during the perturbation are used which is the part that is greyed out in Figure 7. The force in the y-direction and the moments in the x-direction and z-direction are improved the most. Moreover, it stands out that the standard deviation of the perturbation trials without IC is higher than for the other trials. This higher standard deviation depicts a wider variety between subjects. Some of the graphs show a reoccurring pattern of the kinetic residual during one gait cycle. This can mainly be seen in Figure 6 for the force in the x and z-direction and the moment in the y-direction. Figure 7 mainly shows this reoccurring pattern for the forces in x and z-direction. Furthermore, Figure 7 shows similar patterns for the uncompensated force in the y-direction and the moment in the x and z-direction.

The mean and standard deviation of all conditions can be seen in Table III. It can be seen that the standard deviation of the pitch trials is relatively big. The raw data for one of the subjects can be seen in Appendix F. It was seen that not all data was normally distributed. The repeated measures two-way ANOVA showed a significant difference between the conditions and IC for all kinetic residuals. The ANOVA test furthermore showed a significant interaction effect between IC and condition. The Friedman's test also showed a significant difference between all conditions and IC for all kinetic residuals. The results for the paired samples t-test and Wilcoxon signed rank test can be seen in Table III. All significant differences are marked with a *. The parametric and non-parametric methods give the same significant differences except for the comparison of sway IC and sway no IC and pitch IC compared to baseline for the force in the x-direction. Also, pitch IC compared to baseline measurement for the moment around the x-axis shows a difference between the two methods. No statistically significant interaction effect was found for gender (p = 0.259, power = 0.184) and length (p = 0.467, power = 0.101). These covariates were therefore left out for the other statistical tests. The power for all conditions and IC was 1.0. The effect size, partial eta squared, was 0.88 or higher.

IV. DISCUSSION

This study aimed to optimize and validate an inertia compensation model for perturbations on instrumented treadmills. It can be concluded that the R-Mill can accurately measure COP, forces and moments. In addition to this, a new calibration trial was found with higher sway accelerations which improved the inertia compensation model. Moreover, it showed that using this inertia compensation model for pitch and sway trials led to a reduction of the kinetic residuals that were close to baseline levels.

A. Dynamic validation

The first part of this study aimed to dynamically validate the force plates of an instrumented treadmill. This resulted in accuracy errors in force between 1-7N, moments between 0.5-4Nm and COP of 1-6mm. These results are comparable to the findings in literature for instrumented treadmills under static conditions [14][23][24][25][26]. Even though the errors in COP are small, it has been shown that 0.5-1.0cm errors in COP can have a big effect on joint kinetics [27]. Most of the studies have only tested accuracy under static conditions while higher errors can be expected under dynamic conditions. It could therefore be concluded that the R-Mill can accurately measure COP, forces and moments.

For the second part of the measurements the results were obtained with metal supports underneath the treadmill to overcome the pitching movements and flexibility of the treadmill. This largely reduced the noise in the COPz signal. RMSE results mainly showed improvements in COPz and furthermore Mx, Fz, Mz and COPx seem to have improved. The improvements in COPz, Mx and Fz are most likely due to a reduction of the pitching moment of the treadmill. The moment around the z-axis and the COPx will most likely be due to less flexibility of the platform in the x-direction.

Differences in error between the different positions on the belt could be due to misalignment of force sensors. The error increase with higher speeds could be explained by a too low capture frequency of the motion capture system. The error for heavier weights was bigger than for the smaller weights. This could be due to the fact that more movement occurred with the heavier weights. Heavier weights could not be used in this set-up because of tripping over of the rod with weights during the high accelerations. The used weights are, however, still quite some lower than the average weight of a subject

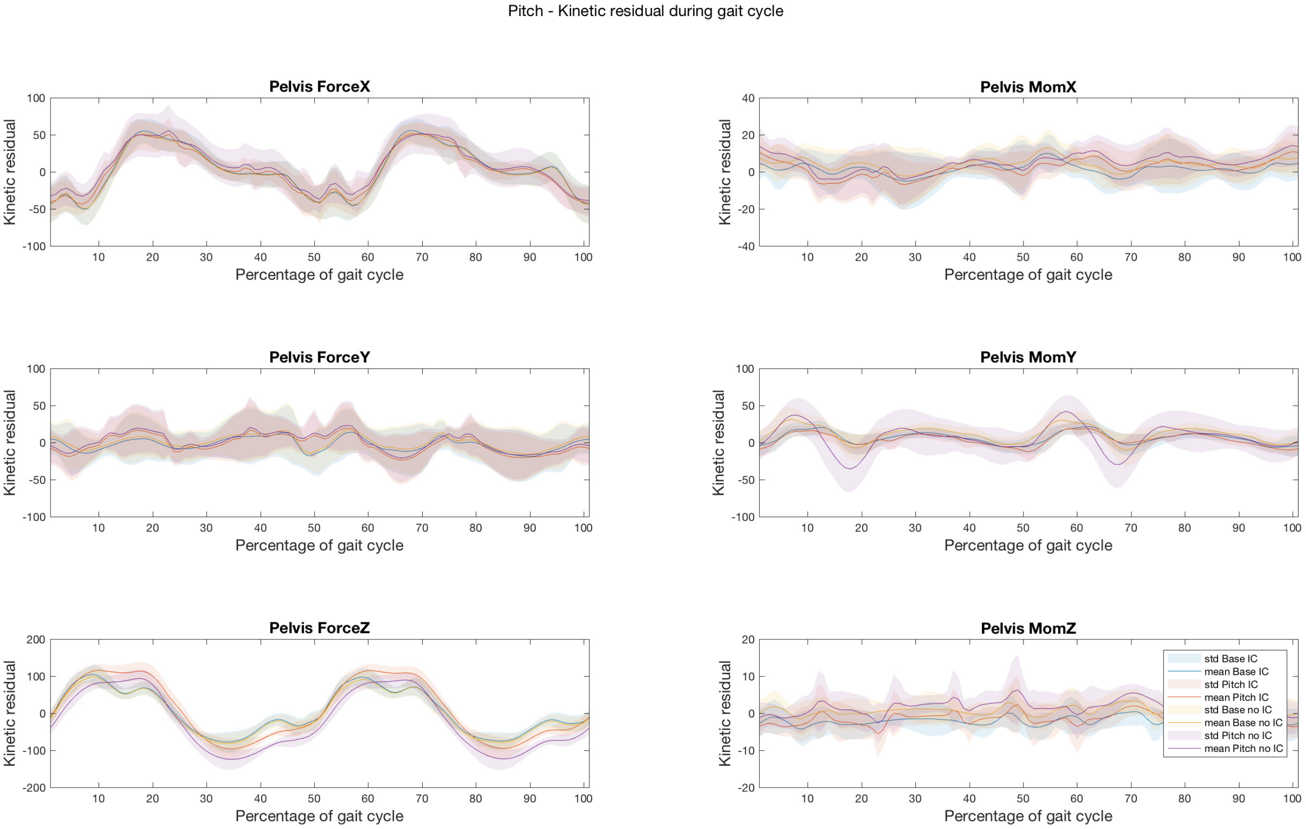

Fig. 6. The mean and standard deviation of the kinetic residuals in time of all subjects during a pitch trial. Data were normalized to a gait cycle. The results for the baseline measurements with and without inertia compensation are compared with the results for the pitch perturbation trials with and without inertia compensation. Please note the different scales on the y-axes.

TABLE III

Mean and standard deviation are shown for all conditions. The difference between IC conditions and baseline condition without IC is shown. The percentage reduction for each condition with and without IC is displayed as well. Results for parametric and non-parametric tests are shown and significant results are marker with a *.

		No IC		**IC**		**IC - Base no IC**	**Reduction**	**Parametric**		**Non-parametric**	
		Mean	Std dev	Mean	St dev	Diff		Sig.	Sig. IC - base	Sig.	Sig. IC - base
Fx (N)	Base	37.1	9.6	38.1	10.0		-2 %	0.000*	-	0.04*	-
	Sway	44.7	10.8	47.4	11.4	9.3	-6 %	0.000*	0.005*	0.055	0.04*
	Pitch	342.0	16.6	74.5	47.8	36.4	78 %	0.000*	0.99	0.04*	0.04*
Fy (N)	Base	30.4	7.0	30.6	7.0		-1 %	0.000*	-	0.04*	-
	Sway	435.5	15.3	33.6	10.1	3.0	92 %	0.000*	1.000	0.04*	0.865
	Pitch	71.7	53.8	71.5	53.9	40.9	0 %	0.000*	1.000	0.04*	0.33
Fz (N)	Base	63.1	11.9	63.3	11.8		0 %	0.340	-	0.550	-
	Sway	62.1	17.0	63.7	15.9	0.3	-3 %	0.065	1.000	0.105	1.000
	Pitch	100.0	15.1	91.0	14.3	27.7	9 %	0.000*	0.000*	0.040*	0.040*
Mx (Nm)	Base	11.4	2.8	10.8	2.6		5 %	0.230	-	0.330	-
	Sway	469.3	34.8	19.5	3.7	8.8	96 %	0.000*	0.005*	0.040*	0.040*
	Pitch	22.9	13.7	21.4	14.1	10.6	7 %	0.000*	1.000	0.040*	0.040*
My (Nm)	Base	20.5	6.7	17.2	3.5		16 %	0.965	-	1.000	-
	Sway	26.9	9.4	22.1	3.2	4.9	18 %	1.000	1.000	1.000	0.695
	Pitch	357.6	33.1	33.9	9.8	16.6	91 %	0.000*	0.800	0.040*	0.055
Mz (Nm)	Base	4.5	1.2	5.1	1.4		-13 %	0.005*		0.040*	-
	Sway	202.1	46.5	13.7	1.4	8.6	93 %	0.000*	0.000*	0.040*	0.040*
	Pitch	22.6	17.3	21.0	17.9	15.9	7 %	0.000*	1.000	0.040*	0.055

that usually walks on the treadmill. Tests with higher weights might therefore give some more insight in the force accuracy. Another experimental error can also be due to a misalignment of the marker on top of the calibrated weight.

Linearity in vertical force resulted in numbers just a little higher than in literature. Where the non-linearity is 6.7N

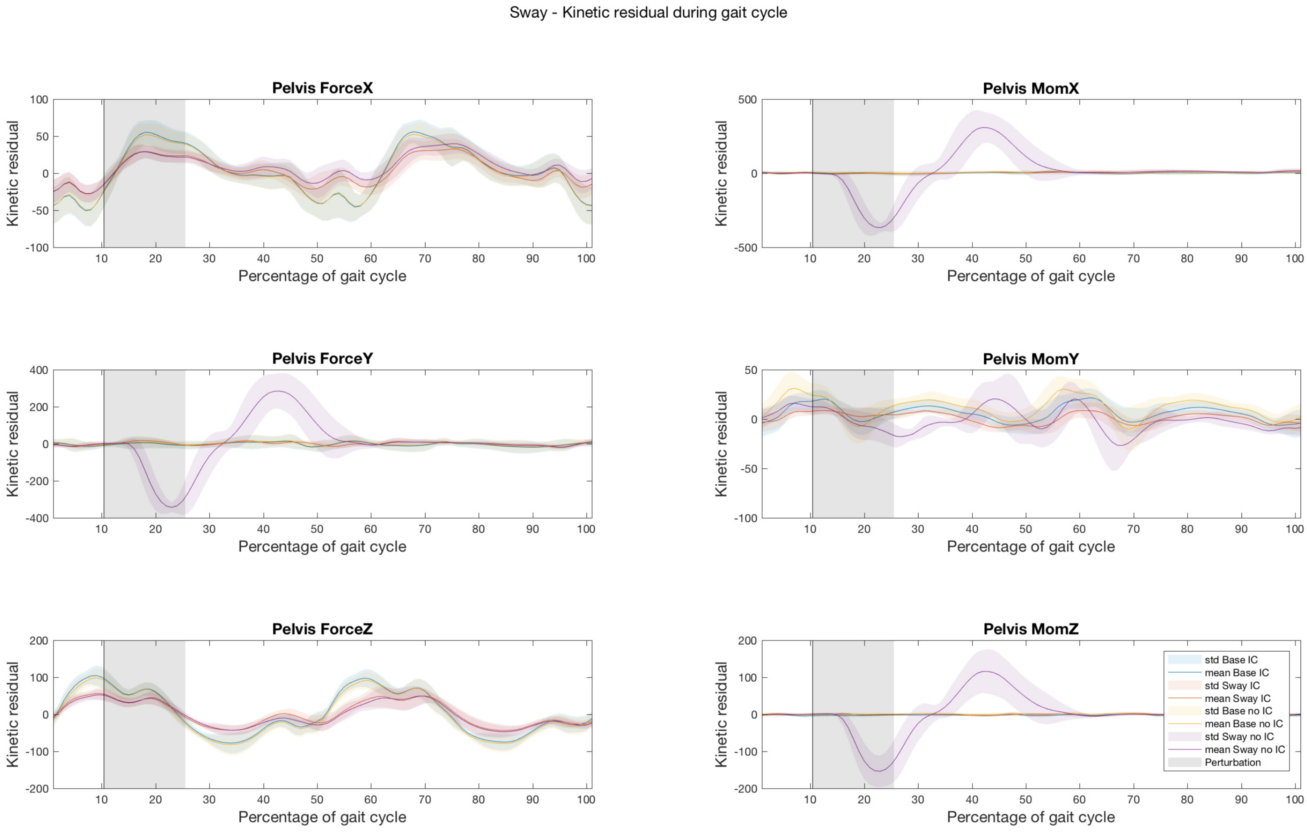

Fig. 7. The mean and standard deviation of the kinetic residuals in time of all subjects during a sway trial. Data were normalized to a gait cycle. The results for the baseline measurements with and without inertia compensation are compared with the results for the sway perturbation trials with and without inertia compensation. Please note the different scales on the y-axes.

(1.3% FSO) in this study, most other studies report values between 2-6N (around 0.3 % FSO).

A delay between force plate data and motion capture data was found of less than a frame of the marker data. Smaller delays were found due to the fact that the force plate data were captured at 1000Hz whereas the marker data were captured at 100Hz. It can be concluded that no measures need to be taken to compensate for the delay.

B. *Optimization of calibration trial*

The aim of the second part of this study was to find the optimal calibration trial for inertia compensation on an instrumented treadmill. This was done for the combination of pitch and sway perturbations and for belt perturbations.

This resulted in a trial with a random signal of pitch and sway perturbations with some square waves of sway added to it. The high accelerations in this trial might be important as those are not yet present in the random signal but are used in real life applications. In some earlier tests it was seen that using a calibration trial without any perturbations at all does improve the inertia compensation. This is probably due to the fact that the IC model can measure the offset as used in the linear model. High accelerations of pitching did not seem to improve the inertia compensation a lot. A reason for this could be that no high accelerations are used in the validation trials and in the real use which makes them less necessary. For the belt perturbations the calibration trial that turned out best was the one with a random signal of belt accelerations and some perturbations similar to normal use. All trials showed very similar results which could mean that the dynamics of the system are captured accurately [15].

Table II shows RMS after compensation for pitch and sway appear to be around 1 N or Nm with a few exceptions of 2 N or Nm. The calibration trial with a random signal of belt accelerations for 60 seconds plus perturbations ended up best in the ranking ($R^2 = 0.97$, RMS raw = $21.60Nm$, RMS compensated $= 3.74Nm$, RMS reduction = 83%). The trial with a square wave of sway in it resulted in a RMS reduction of up to 99%. This is comparable to results that are commonly accepted for gait analysis [16][28]. Results of dynamic and static validation of force plates show similar results as well [14][25].

Concerning the belt speed during the calibration trial no significant differences were found in belt accelerations. For pitch and sway perturbations 3 m/s turned out to be better than a belt speed of 0 m/s. This could be due to some vibrations caused by the rotating motors at higher speeds. The accelerometers are able to pick up some of this and can compensate for these vibrations. The difference between a duration of 300 seconds and one of 60 seconds was quite small. The longer duration turned out to be a bit better but will also cost more time during calibration. Therefore, a longer trial can be used but it is not necessary.

Future research could focus on optimizing the calibration trial even further by looking at more different durations and speeds.

C. Evaluation of a musculoskeletal model with inertia compensation

The aim of the third part of the study was to evaluate the effect of inertia compensation on the outcomes of a musculoskeletal model. This experiment resulted in a high reduction of certain kinetic residuals of up to 96% as can be seen in Table III. The difference between baseline measurements and the results with inertia compensation can be seen as the error of the musculoskeletal model during perturbations. This error might be caused by an error of the inertia compensation model. It can also be due to a change in movement of the subject during perturbations. Such movements might result in biomechanics that are more difficult to capture for the musculoskeletal model and thereby increase kinetic residuals. The differences between baseline without IC and sway with IC kinetic residuals range between 2 and 10N(m). The differences between baseline without IC and pitch with IC kinetic residuals range between 6 and 28N(m). Inertia compensation leads to a high reduction of the kinetic residuals which can largely improve the use of a musculoskeletal model during perturbations. A relatively high standard deviation can be seen for the pitch trials. This could indicate a different response of IC for different subjects.

The amount of reduction due to inertia compensation differs between conditions and kinetic residuals. Part of this can be prescribed to the fact that for some kinetic residuals little inertial and gravitational artifacts occur. The IC model cannot compensate whenever no inertial and gravitational artifacts occur and therefore has little effect. The gravitational and inertial artifacts of a pitching trial can clearly be seen in Figure 3. Two different coordinate systems are used, one for the force plate measurement itself and one for the kinetic residuals. When compensating for this difference it can be seen that the biggest compensation is indeed for the directions with the highest inertial and gravitational artifacts. During sway perturbations for example, a movement with a high acceleration is performed in the y-direction. The percentage reduction of the kinetic residual is high for the force in the y-direction, as would be expected. Reoccurring patterns can be seen in Figure 6 and 7. Part of this can be due to the fact that the same kinetic residuals occur during both the left and the right step. A reoccurring pattern can also be found because of a difference between the sway and swing phase.

The kinetic residuals of the baseline measurement range between 29 and 62N for the forces and between 4 and 20Nm for the moments. These results are a little higher than in literature but are still less than 10% of the total force of around 600N (75kg) exerted by the subjects. Differences with other studies can partly be explained by other length to mass ratios of the subjects. Reasons for high residuals could be inaccurate marker placement, soft tissue artifacts due to movement of the skin with markers and the estimation of the human dimensional and inertial parameters. The results might also be improved by compensating for the misalignment between the motion capture coordinate system and the force plate coordinate system, as is done in experiment 1. The walking speed was kept the same for all subjects in this study. This might lead to higher residuals than when using a walking speed normalized to leg length. Different walking speeds cause different biomechanics which might in turn lead to these higher residuals. Furthermore, the kinetic residuals might be lowered with a better visual flow during the pitch measurements. The visual flow in this study was not entirely natural which can cause differences in gait pattern. The power of the study was high because of the large effect size between with and without IC. Length and gender did not seem to influence the effect of IC but had low power. A larger amount of subjects with more variation in length and height might give an even better insight in the effect of the IC model. Future research could also focus on looking at the effects of IC on the muscle force and power. Directly comparing the joint moments and forces to for example pressure insoles might give more insight in the effect as well.

Overall can be concluded that the effect of inertia compensation on the outcomes of the musculoskeletal model are high. Some difference between baseline measurement and perturbations measurements with IC still remains but the differences are low and the error is probably not entirely due to the IC model. The IC model can therefore enable and greatly improve force measurement during perturbations.

ACKNOWLEDGMENT

This study was supported by Motekforce Link (Amsterdam) and the Biomedical Engineering department of the TU Delft for which we want to express our gratitude. We also want to thank all participants for helping out during the measurements.

REFERENCES

[1] Morin, J. B., Edouard, P., & Samozino, P. (2011). Technical ability of force application as a determinant factor of sprint performance. Medicine and science in sports and exercise, 43(9), 1680-1688.

[2] Tesio, L., & Rota, V. (2008). Gait analysis on split-belt force treadmills: validation of an instrument. American journal of physical medicine & rehabilitation, 87(7), 515-526.

[3] Van den Bogert, A. J., Geijtenbeek, T., Even-Zohar, O., Steenbrink, F., & Hardin, E. C. (2013). A real-time system for biomechanical analysis of human movement and muscle function. Medical & biological engineering & computing, 51(10), 1069-1077.

[4] Pizzolato, C., Reggiani, M., Modenese, L., Lloyd, D. G. (2017). Real-time inverse kinematics and inverse dynamics for lower limb applications using OpenSim. Computer methods in biomechanics and biomedical engineering, 20(4), 436-445.

[5] Sessoms, P. H., Wyatt, M., Grabiner, M., Collins, J. D., Kingsbury, T., Thesing, N., & Kaufman, K. (2014). Method for evoking a trip-like response using a treadmill-based perturbation during locomotion. Journal of biomechanics, 47(1), 277-280.

[6] van den Noort, J. C., Sloot, L. H., Bruijn, S. M., & Harlaar, J. (2017). How to measure responses of the knee to lateral perturbations during gait? A proof-of-principle for quantification of knee instability. Journal of biomechanics, 61, 111-122.

[7] Silva, M. P., & Ambrsio, J. A. (2004). Sensitivity of the results produced by the inverse dynamic analysis of a human stride to perturbed input data. Gait & posture, 19(1), 35-49.

[8] Pmies-Vil, R., Font-Llagunes, J. M., Cuadrado, J., & Alonso, F. J. (2012). Analysis of different uncertainties in the inverse dynamic analysis of human gait. Mechanism and machine theory, 58, 153-164.

[9] Hicks, J. L., Uchida, T. K., Seth, A., Rajagopal, A., & Delp, S. L. (2015). Is my model good enough? Best practices for verification and validation of musculoskeletal models and simulations of movement. Journal of biomechanical engineering, 137(2), 020905.

[10] Lund, M. E., de Zee, M., Andersen, M. S., & Rasmussen, J. (2012). On validation of multibody musculoskeletal models. Proceedings of the Institution of Mechanical Engineers, Part H: Journal of Engineering in Medicine, 226(2), 82-94.

[11] Merriaux, P., Dupuis, Y., Boutteau, R., Vasseur, P., & Savatier, X. (2017). A study of Vicon system positioning performance. Sensors, 17(7), 1591.

[12] Sloot, L. H., Houdijk, H., & Harlaar, J. (2015). A comprehensive protocol to test instrumented treadmills. Medical engineering & physics, 37(6), 610-616.

[13] Aarts, L., Papegaaij, S., Steenbrink, F., & Martens, P. (2018). Quality of treadmill embedded force plates for gait analysis.

[14] Fortune, E., Crenshaw, J., Lugade, V., & Kaufman, K. R. (2017). Dynamic assessment of center of pressure measurements from an instrumented AMTI treadmill with controlled precision. Medical engineering & physics, 42, 99-104.

[15] Hnat, S. K., & Van den Bogert, A. J. (2014). Inertial compensation for belt acceleration in an instrumented treadmill. Journal of Biomechanics, 47(15), 3758-3761.

[16] Hnat, S. K., van Basten, B. J., & van den Bogert, A. J. (2018). Compensation for inertial and gravity effects in a moving force platform. Journal of biomechanics.

[17] Moore, J. K., Hnat, S. K., & van den Bogert, A. J. (2015). An elaborate data set on human gait and the effect of mechanical perturbations. PeerJ, 3, e918.

[18] Goldberg, S. R., Kepple, T. M., & Stanhope, S. J. (2009). In situ calibration and motion capture transformation optimization improve instrumented treadmill measurements. Journal of applied biomechanics, 25(4), 401-406.

[19] Markovsky, I., & Van Huffel, S. (2007). Overview of total least-squares methods. Signal processing, 87(10), 2283-2302.

[20] Petr, I., & Bednrov, D. (2010). Total least squares approach to modeling: a Matlab toolbox. Acta Montanistica Slovaca, 15(2), 158.

[21] Woltring, H.J. (1986, May 12). GCVSPL software package [Memorandum]. Philips Medical Systems Division, Eindhoven, University of Nijmegen (The Netherlands). Retrieved from http://isbweb.org/software/sigproc/gcvspl/gcvspl.memo

[22] Bohannon, R. W. (1997). Comfortable and maximum walking speed of adults aged 2079 years: reference values and determinants. Age and ageing, 26(1), 15-19.

[23] Tesio, L., & Rota, V. (2008). Gait analysis on split-belt force treadmills: validation of an instrument. American journal of physical medicine rehabilitation, 87(7), 515-526.

[24] Paolini, G., Della Croce, U., Riley, P. O., Newton, F. K., & Kerrigan, D. C. (2007). Testing of a tri-instrumented-treadmill unit for kinetic analysis of locomotion tasks in static and dynamic loading conditions. Medical engineering & physics, 29(3), 404-411.

[25] Sloot, L. H., Houdijk, H., & Harlaar, J. (2015). A comprehensive protocol to test instrumented treadmills. Medical engineering & physics, 37(6), 610-616.

[26] Bobbert, M. F., & Schamhardt, H. C. (1990). Accuracy of determining the point of force application with piezoelectric force plates. Journal of Biomechanics, 23(7), 705-710.

[27] McCaw, S. T., & DeVita, P. (1995). Errors in alignment of center of pressure and foot coordinates affect predicted lower extremity torques. Journal of biomechanics, 28(8), 985-988.

[28] Lloyd, D. G., & Besier, T. F. (2003). An EMG-driven musculoskeletal model to estimate muscle forces and knee joint moments in vivo. Journal of biomechanics, 36(6), 765-776.

A

Dynamic validation

A.1. Force measurements

The force plates in this study consist of six force sensors each. The set-up and specifications of the R-Mill and its force plates can be seen in Figure A.1. The force sensors are electrical sensors that output a voltage which changes by applying a force to it. A calibration matrix is set up to convert these voltages into forces. This calibration is done by placing calibrated weights with a marker on it on the force plates. The error between the forces as measured by the force plates and the forces exerted by the weights is then minimized. The weights were then calculated using this calibration matrix [1]:

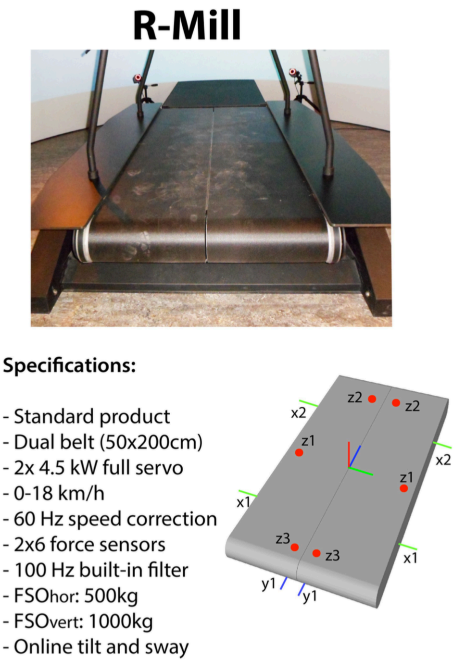

Specifications:

- Standard product
- Dual belt (50x200cm)
- 2x 4.5 kW full servo
- 0-18 km/h
- 60 Hz speed correction
- 2x6 force sensors
- 100 Hz built-in filter
- FSOhor: 500kg
- FSOvert: 1000kg
- Online tilt and sway

Figure A.1: Specifications of the R-Mill and its force plates [1].

$$F = (S_V - Offset_V) * C \tag{A.1}$$

In which F are the forces and moments, S_v the voltage measured by the force sensors, the $Offset$ is the voltage measured without any load on it and C is the calibration matrix. The center of pressure can be obtained from the forces and moments:

$$COP_{ml} = \frac{F_{ml} COP_v + M_{ap}}{F_v} \tag{A.2}$$

where F is the force, M the moment, ml is mediolateral, v is vertical and ap is anterior posterior. The COP_v is the distance between the force sensors and the surface of the belt. The same procedure can be followed to calculate the centure of pressure in the anterior posterior direction.

A.2. Error in dynamic force plate measurements

Errors in instrumented treadmill measurements can arise from different parts of the treadmill. The calculation for the centre of pressure and the forces itself are based on the voltages as obtained from six different force sensors per force plate. A wrong calibration of the force sensors could therefore lead to errors in the COP, as could wrong measurements of one of the sensors. Other sources of errors can be mistakes in the mounting of force sensors and from some flexibility of the force plate. The stiffer the force plate will be, the better the results. Weight of the force plates in instrumented treadmills is limited and therefore it can be harder to obtain the same result of stiffness as in normal, overground force plates. Consequently, higher errors can be expected than in normal force plates. Movements of the platform and thus the force plates could also reduce accuracy. The motion capture system can produce an error by either mistakes in one of the cameras of the system or in the calculations of the marker position. It has, however, been shown that even under dynamic circumstances the Vicon motion capture system as used in this study showed less than 2mm error [2].

Static validations of force plates are done regularly. Dynamic evaluation is less common and is therefore described in this paper. A static validation has been done for Motekforce Link's R-Mill as described in an earlier paper [3]. As the force plates in the treadmill are often used under dynamic circumstances, testing during these conditions seems necessary to be able to discuss the quality of the treadmill. Some of the parameters measured during static validation will not change under dynamic circumstances and are therefore not tested. The parameters that are tested are the accuracy (Section A.3) and linearity (Section A.4). Furthermore, the delay (Section A.5) between the force plates and markers was obtained. All of these parameters are discussed below.

A.3. Accuracy

Accuracy is measured for two different properties; the magnitude of the force and the position of the measured force. Where the latter can be called the center of pressure or COP. Marker positions and accelerations and calibrated weights are used to validate the force plates, as is done more often in literature. The accuracy error for the COP can then be defined as the difference between the COP measured by the force plates and the COP measured by the motion capture system [1][4]. The calibrated weights are used to validate the magnitude of the forces. Force accuracy error was in turn determined as the difference between measured force and the applied known load. A combination of the accelerations of the marker and the calibrated weight were used as a golden standard for force accuracy.

In a dynamic assessment of an instrumented treadmill, Fortune et al. (2017) showed that COP precision is speed dependent [5]. Therefore, different speeds are tested in this study. Next to this, acceleration and different positions on the force plate may have influence on accuracy. There might be a difference between the two force plates which is tested for as well. It is, however, expected that no differences in both COP and force accuracy will be found between these different speeds, accelerations, positions and weights.

A.4. Linearity

Linearity in force measurement means that by multiplying a given load with a certain factor, the corresponding measured load is multiplied by the same factor. Non-linearity is seen as the maximum deviation from a linear least squares regression of the measured forces versus the known forces. This maximum deviation was defined as three standard deviations, in order to remove outliers [1][6]. Fortune et al. (2017) showed that in their dynamic assessments the treadmill was non-linear in measuring forces [5]. If the non-linearity is high, the force plate can be accurate for some weights but inaccurate for other weights. This can result in incorrect kinetic data.

A.5. Delay

Delay is in this case seen as the difference between the moment at which marker data are obtained and the moment at which the corresponding force plate data are obtained. A delay could originate from e.g. the time it takes to pass through the wires and the computational time to calculate forces and moments from the voltages obtained by the force sensors in the force plate. Vicon does allow for synchronization of the force plate and motion capture system data already during configuration but it has not yet been checked for this set-up [7]. It is expected that the delay is less than a frame. As the data of the marker data and force plate data are compared and used to calculate the accuracy, a delay between those two can potentially induce a higher error. Compensating for this delay could overcome this.

A.6. Static calibration

Part of a COP error could also be due to an incorrect calibration of the motion capture system relative to the force plates. In the GRAIL set up, the cameras are not rigidly attached to the treadmill and thus to the force plate. Because of this, the coordinate systems of the force plates and of the motion capture system need to be aligned manually before testing. Before starting the measurement, this was done using an active wand with markers that was mounted to the treadmill. Even though this was done, a minor misalignment during calibration could lead to larger COP errors at the outer edges of the treadmill. Therefore, a compensation was done as proposed by Goldberg et al. (2009) [8].

B

Human Body Model

The model used in this study was the Human Body Model version 2.0 which is an improved version of the original model [9]. A full body marker set with 46 markers was used.

B.1. Numerical methods

The pipeline of the Human Body Model consists of measuring the markers and forces, defining a skeleton, inverse kinematics, inverse dynamics and calculating muscle forces. The model uses 46 markers and has 46 degrees of freedom and 18 segments. The pelvis is taken as the base segment. The pelvis has a reference frame that can be described relative to the world with six degrees of freedom. The reference frames of the other segments are calculated during an initialization pose (Tpose) of the subject. During this time the individual joint axes and center are calculated with the help of the markers. The origin of a segment is defined to be in the proximal joint and the Z-axis is the axis that goes through the distal joint, according to De Leva (1996) [10]. The rotations are according to clinical definitions. The segment masses are also calculated during initialization pose. These calculations are based on body mass, segment lengths and gender. This information is combined with the anthropometric data of De Leva (1996) from which the segment mass properties are calculated [10]. Some of the 46 markers are not placed at anatomical landmarks but do provide robustness. The place of these markers in the local reference frames is known from the initialization. The extra markers can thereby reduce the error when other markers go missing. The entire pipeline of the Human Body Model can be seen in Figure B.1

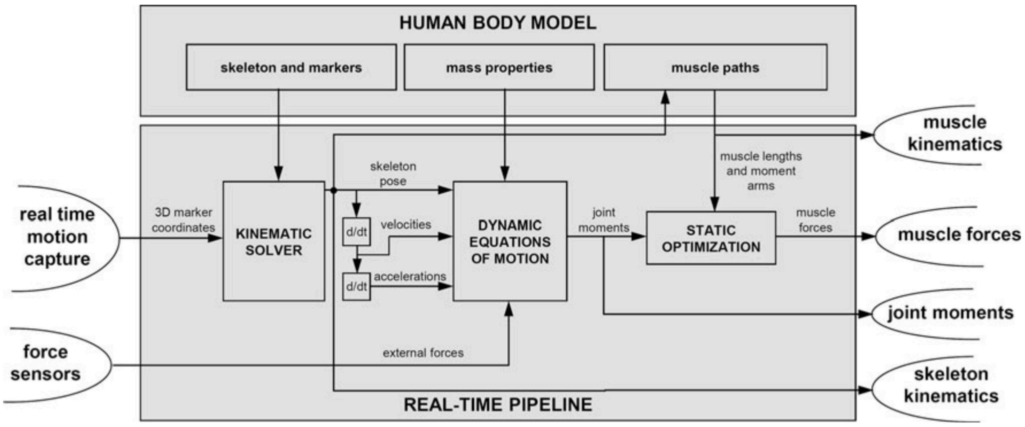
HUMAN BODY MODEL
skeleton and markers
mass properties
muscle paths
muscle kinematics
skeleton pose
muscle lengths and moment arms
real time motion capture
3D marker coordinates
KINEMATIC SOLVER
d/dt
velocities
DYNAMIC EQUATIONS OF MOTION
joint moments
STATIC OPTIMIZATION
muscle forces
muscle forces
d/dt
accelerations
joint moments
force sensors
external forces
skeleton kinematics
REAL-TIME PIPELINE

Figure B.1: The pipeline of the Human Body Model [9].

B.1.1. Inverse kinematics

The goal of the inverse kinematics is to find the skeletal pose that best fits the marker data. Calculations for this have to be done fast as the HBM can be used in real-time as well. Therefore, the optimization to find the best model pose is done all at once, so for the entire body. Many models start by calculating the optimal pose of the ankle and from there on build the rest of the skeleton. Calculating all segments separately is slower and also increases the error the further the calculation goes as it uses the data of the previous segments and their corresponding errors.

The segment position is calculated by minimizing the error between the measured marker positions and the position of the markers expressed as a function of the segment positions. The model pose is defined as q and all degrees of freedom are associated with generalized coordinates $q = [q_1 ... q_{46}]$.

The model pose q is thus optimized using the least squares problem:

$$q = arg\min_q \sum_{i=1}^{N} ||\vec{r_i}(q) - \vec{r}_{i,meas}||^2 \tag{B.1}$$

Where N is the amount of markers used, $r_{i,meas}$ are the measured positions of the markers in the global reference frame and $r_i(q)$ are the marker positions in the global reference frame expressed as a function of the segment positions. This last part can be calculated by adding the position of the origin of the reference frame to the position of the markers. The remainder of this optimization problem are the kinematic residuals and can be seen as a measure of goodness of the model.

Before the next step of inverse kinetics, the generalized positions need to be filtered and differentiated. The HBM uses a 2^{nd} order low-pass Butterworth filter to smooth the position data. Filters with a higher order might give better results but will also increase time delay which is unfavourable as this filtering is done in real-time. The filter is a state variable filter which allows for sample rate variability which can appear with marker drop out. A cut-off frequency can be set of up to 20Hz and has a typical value of 6Hz for gait analysis. The same filter was used for processing the force data to prevent artifacts in joint movements. The generalized velocity $\dot{q}$ and acceleration $\ddot{q}$, being the first and second derivative of the position, are used for the calculation of joint moments and forces.

B.1.2. Inverse dynamics

The goal of inverse dynamics is to find the forces and moments for each degree of freedom. Each degree of freedom is, in addition to being associated with generalized coordinates, associated with a force or moment. These 'generalized forces' are defined in such a way that an increase in force belongs to an increase in the generalized coordinate that corresponds to the force. The calculation of these forces use the filtered kinematics and ground reaction forces. This analysis is called an inverse dynamic analysis and is done using the following formula:

$$\tau = M(q)\ddot{q} + c(q, \dot{q}) + B(q)\tau_{ext} \tag{B.2}$$

Where τ is a vector of internal unknown torques and moments, M is the mass matrix, c are the terms that have to do with gravity, centrifugal and Coriolis effect and $B(q)\ \tau_{ext}$ are the external measured forces from the force plate.

B.1.3. Muscle forces

Muscle forces and power can also be calculated using the Human Body Model. The HBM comprises a total of 300 muscles. The lower extremities contain 43 muscles, the arms 102 and the spine another 10 muscles. The maximal isometric force per muscle is available from cadaver data and is together with joint kinematics used to calculate muscle force. No in depth explanation of this topic will be given here as the muscle forces are outside the scope of this paper.

B.2. Kinetic residuals

While calculating the kinetics, a certain part of the forces is described to the pelvis even though this is the root joint and zero forces would be expected here. The forces described to the pelvis are the forces that are still left when prescribing forces to all other generalized coordinates. These forces and moments, or kinetic residuals, can therefore be seen as the error of the model [11][12]. The lower the kinetic residuals, the better the model could prescribe all forces and moments to the joints.

High kinetic residuals can be a result of an inaccurate musculoskeletal model but can also be due to experimental errors. Errors in the model can for example arise from assumptions that are made about the segment masses and their positions. Moreover the model assumes that the same model can be used for all subjects with only taking gender and segment lengths into account. Inaccuracies can also originate from soft tissue artifacts because of marker movement. In literature, several different methods are used to reduce the kinetic residuals like adjusting the paths of the markers [13][14].

In the Human Body Model the kinetic residuals are expressed in the global reference frame. The reference frame of the pelvis can therefore be described with six degrees of freedom relative to the world. In this frame the x-axis is defined anterior posterior with forward being positive. A rotation around the x-axis is called pelvic roll and is defined positive when the left part is lifted. The y-axis is mediolateral and positive to the right. Rotation around this axis is defined as pelvic pitch with backward pitch being positive. The z-axis points upwards and has a rotation around it that is called pelvic yaw which is defined positive when twisting left.

C

Inertia compensation model

The forces as used by HBM are calculated from twelve force sensors on the force plate and uses an input device configuration file to do so. This file consists of a matrix by which the analog force sensor signals are multiplied and is based on a calibration of the force plates. This results in accurate force measurements with a static treadmill as was proven in experiment 1. However, while the entire treadmill is moving it measures inertial and gravitational forces that are not induced by a subject on the treadmill. To overcome this, a model has been made that changes the forces before giving them to the musculoskeletal model in such a way that they are more accurate while moving.

C.1. Dynamics of the inertia compensation method

The treadmill that is used has two degrees of freedom: rotation around the x-axis and translation in the direction of the x-axis. For the inertia compensation method that is used in this study a model is used that is a linear relation between the forces as measured by the treadmill and the accelerations as measured by the accelerometers. The equations of motion are described below to show that this equation is valid. A set-up of the treadmill with the acceleromter and force plates can be seen in Figure C.1. A free body diagram of the treadmill can be seen in Figure C.2

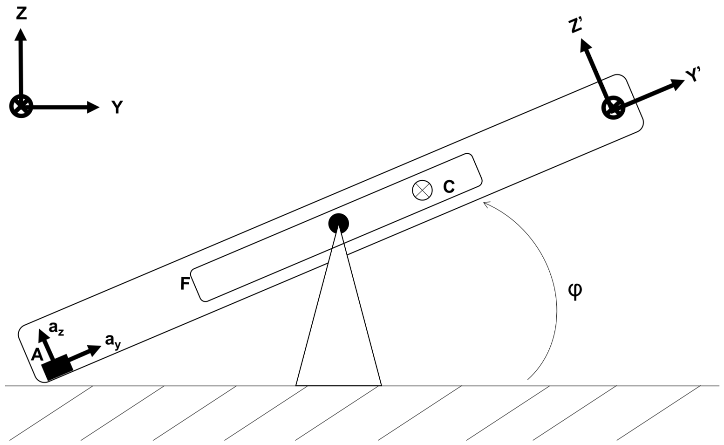

Figure C.1: Set-up of the treadmill with C the center of mass, F the force plate, A the accelerometer and τ the pitch angle between the floor and the treadmill. The Z-Y coordinate system is a global coordinate system and the Z′-Y′ coordinate system is a local reference system.

Inertial frame N belongs to coordinate system XYZ with origin O. Body fixed frame B is associated with coordinate system x′y′z′ with origin o′. This origin lies on the X-axis. The forces measured by the force plate as well as the accelerations measured by the accelerometers will both be in the body-fixed frame. Therefore, all other equations will be expressed in the body-fixed frame.

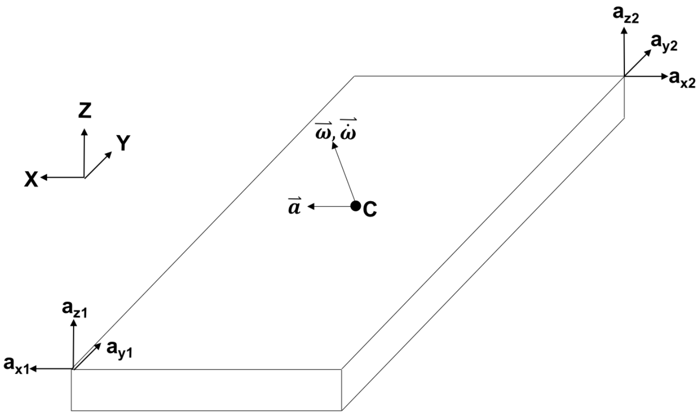

Figure C.2: Free body diagram of the treadmill with C the center of mass, ω and $\dot{\omega}$ the angular velocity and acceleration and a the accelerometer accelerations.

The center of mass (COM) lies in point C and is body-fixed. It is assumed that point C lies on the z′-axis as the weight will most likely be equal in x′ and y′ direction. In z′ direction it will most likely not be equal as the motors are placed in the back of the belt. It is also assumed that there is no motion relative to the rotating, so the body fixed, frame. Meaning that the center of mass stays at the same position during movement. The position vector between o′ and C is referred to as $\underline{\rho}$. The position vector between O and C is referred to as $\underline{R}$. The X-axis aligns with the pitch axis and the angle is ϕ. Sway is motion along the X-axis. In the body fixed frame, for point C the sum of all torques equals the rate of change of angular momentum:

$$\sum M_C^B = \dot{H}_C^B \tag{C.1}$$

The angular velocity vector is referred to as $\underline{\omega}$ and defined as

$$\omega^B = \omega^N = \begin{pmatrix} \dot{\phi} \\ 0 \\ 0 \end{pmatrix} \tag{C.2}$$

The inertia tensor I is assumed constant in the body-fixed frame.

$$I^B = \begin{pmatrix} I_{x'x'} & I_{y'x'} & I_{z'x'} \\ I_{x'y'} & I'_{y'y'} & I_{z'y'} \\ I_{x'z'} & I_{y'z'} & I_{z'z'} \end{pmatrix} \tag{C.3}$$

The sum of moments in the body-fixed frame is then given by the following equation:

$$\sum M_C^B = \dot{H}_C^B = \frac{d}{dt}(I\omega) = \dot{I}\omega + I\dot{\omega} = \ddot{\phi} \begin{pmatrix} I_{x'x'} \\ I_{x'y'} \\ I_{x'z'} \end{pmatrix} \tag{C.4}$$

Where H is the angular momentum and the derivative of the inertia tensor is zero as it is constant. As the angular acceleration is only around the x-axis, the inertia tensor can be reduced to a vector of inertial terms for the x-axis.
The sum of forces in the body fixed frame can be calculated using the second law of Newton. The acceleration then consists of the linear acceleration, tangential acceleration, the centrifugal acceleration, the coriolis acceleration and gravity.

$$\sum F_C^B = ma_C^B = m(\ddot{R}^B + \dot{\omega}^B \times \rho^B + \omega^B \times (\omega^B \times \rho^B) + ((\ddot{\rho})_B + 2\omega \times (\dot{\rho})_B + g) \tag{C.5}$$

Assuming that point C lies on the z'-axis and there is no motion of C in the body-fixed frame the equation becomes.

$$\sum F_C^B = m(\begin{pmatrix} \ddot{R}_x \\ 0 \\ 0 \end{pmatrix} + \begin{pmatrix} \ddot{\phi} \\ 0 \\ 0 \end{pmatrix} \times \begin{pmatrix} 0 \\ 0 \\ R_x \end{pmatrix} + \begin{pmatrix} \dot{\phi} \\ 0 \\ 0 \end{pmatrix} \times (\begin{pmatrix} \dot{\phi} \\ 0 \\ 0 \end{pmatrix} \times \begin{pmatrix} 0 \\ 0 \\ R_x \end{pmatrix} + 0 + 0 + g \begin{pmatrix} 0 \\ sin(\phi) \\ cos(\phi) \end{pmatrix}) \tag{C.6}$$

$$= m(\begin{pmatrix} \ddot{R}_x \\ -\ddot{\phi} R_x \\ -\dot{\phi}^2 R_x \end{pmatrix} + g \begin{pmatrix} 0 \\ sin(\phi) \\ cos(\phi) \end{pmatrix}) \tag{C.7}$$

However, accelerometer signals are used in the IC model instead of tilt angles and their derivatives. The relationship between these two can be described using the tangential and normal acceleration.

$$\ddot{\phi} = \frac{a_z}{R} \tag{C.8}$$

$$\dot{\phi}^2 = \frac{a_y}{R} \tag{C.9}$$

$$a_z = g * sin(\phi) \tag{C.10}$$

$$a_y = g * cos(\phi) \tag{C.11}$$

Inserting these equations into Equation C.4 and C.7 then gives:

$$\sum M_C^B = \frac{a_z}{R} \begin{pmatrix} I_{x'x'} \\ I_{x'y'} \\ I_{x'z'} \end{pmatrix} \tag{C.12}$$

$$\sum F_C^B = m(\begin{pmatrix} a_x \\ -a_z \\ -a_y \end{pmatrix} + \begin{pmatrix} 0 \\ a_y \\ a_z \end{pmatrix}) \tag{C.13}$$

Both the forces and moments of the COM in the body-fixed frame are linearly related to the accelerations as measured by the accelerometers.

D

Methods

D.1. Dynamic validation

The treadmill (Motekforce Link's R-Mill with a Vicon motion capture system) was tested under several different circumstances. First of all, a distinction was made between constant treadmill speed and acceleration. Three different speeds were measured (0.3m/s, 0.7 m/s and 1.0m/s) and four different weights were used (13.44kg, 22.56kg, 36.00kg and 45.08kg). Also, all of the above were measured for three different mediolateral positions per belt and two different speed profiles.

In order to do so, a test set-up was created in which weights of approximately 4.5kg were piled on a rod as can be seen in Figure D.1. A reflective marker was placed on top of the rod (in the middle of the weight) to enable COP measurements with the motion capture system. The weights were then placed 25 cm from the front of the treadmill and moved to the back of the treadmill by running the belts. At the moment the weights were moved backwards for approximately 1.5m, they were returned to the front again and the same procedure was repeated. This was done three times for each trial.

Six different starting positions in mediolateral direction were chosen, three for each belt, as can be seen in Figure D.2. Two different types of speed profiles were used, a sine and a square wave. The first to obtain acceleration data and the second to obtain constant speed data. Both of them were run with a maximum acceleration of $4.0m/s^2$. This was done for three different speeds: $0.3m/s$, $0.7m/s$ and $1.0m/s$. The different speed profiles can be seen in Figure D.3.

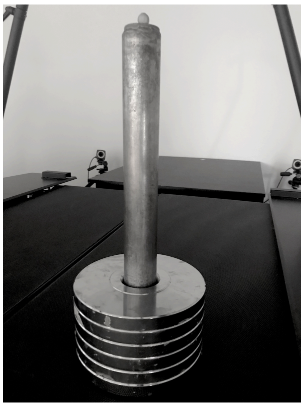

Figure D.1: Set-up of the weights with the marker on top of it.

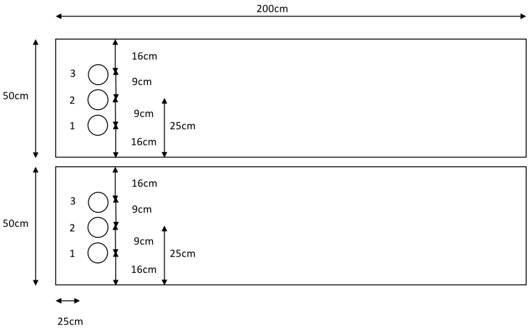

Figure D.2: Top view of the treadmill. The circles represent the different starting positions.

D.1.1. Data acquisition

All marker data has been obtained at 100Hz using the D-Flow software. All force plate data was obtained at 100Hz and synchronized with the marker data from D-Flow. All data for the delay measurements was obtained directly from Vicon with 1000Hz.

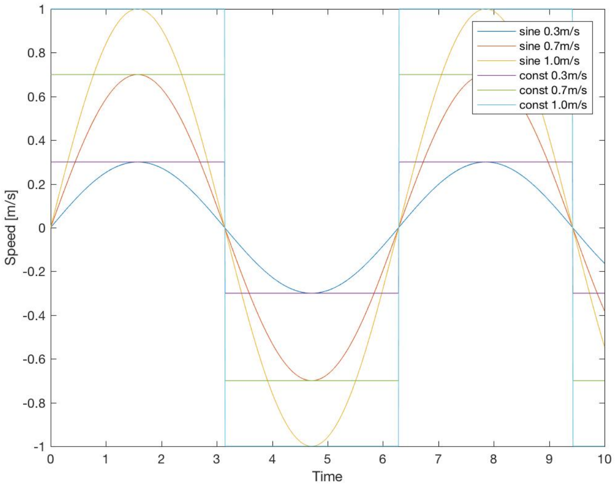

Figure D.3: Different speeds and speed profiles. A negative speed depicts the belt running backwards.

D.1.2. Static calibration

For the static calibration, data was obtained by placing a weight with a marker in the middle on 55 different positions per belt. Both COP data from the force plate and marker data were gathered. Next, an optimization of equation D.1 was done to obtain the best rotation matrix (R) and offset (O). This was then used in the dynamic validation to rotate and offset the marker data.

$$C = arg \min_{C} \sum_{n=1}^{110} (P_{FP} - (P_{marker} * R + O)^2 \tag{D.1}$$

The best rotation matrix and offset were then used to transform the data for the dynamic validation as in equation D.2.

$$P_{marker-corrected} = R^{-1}(P_{marker-original} - O) \tag{D.2}$$

D.1.3. Accuracy

To determine accuracy, the measurements were done as described above and motion and force data were captured. Accuracy of the force was calculated as the the root mean square error between the vertical measured force and the known applied force. This error was calculated for each frame of each trial.

$$RMSE = \sqrt{\frac{\Sigma(F_{FP} - F_{marker+weights})^2}{n}} \tag{D.3}$$

Where F_{FP} is the force plate data, F_{known} are the forces calculated from the marker data and calibrated weights and n is the sample size. The known applied force was determined as the known weight times the acceleration which was in turn differentiated twice from the marker position.

Accuracy of the COP was then calculated in two different ways, both using the root mean square error per frame. The two methods differ in the way the total error is calculated. In literature the total error is most often calculated by taking the difference between the marker data and the COP measured by the force plate. A disadvantage of this being the fact that errors in the marker data are not taken into account. The motion capture system can, however, contain mistakes which could lead to worse results which cannot be entirely prescribed to the force plate. Therefore, the second method uses Total Linear Least Squares (TLLS) which has the advantage that it can take into account the error in both variables [15]. Compared to the ordinary least squares, TLLS calculates the orthogonal distance to the fit instead of the vertical distances as can be seen in Figure D.4. The TLLS calculations were done in Matlab with the singular value deposition method and a Matlab Toolbox was used as basis [16].

The mean RMSE was calculated per trial for each variable (COP_x, COP_y, COP_z, F_x, F_y, F_z, M_x, M_y and M_z) . In this way 144 (2 belts x 3 speeds x 2 speed profiles x 3 starting positions x 4 weights) RMSE's

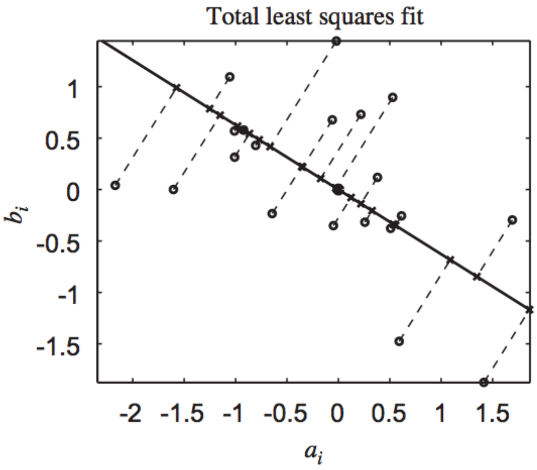

Figure D.4: A total linear least squares fit between the parameters a and b. The total linear least squares fit uses the orthogonal distance to the fit. Figure from Markovskya & Van Huffel (2007)[15].

per variable were obtained. The mean of the RMSE's for each starting position was taken, leading to one RMSE for each starting position, in order to see if differences occurred between ML positions. The same was done for three AP positions, all speeds, speed profiles, weights and the two belts.

D.1.4. Linearity

For linearity, all measurements were performed with different weights, increasing from 13.44kg to 22.56kg to 36.00kg to 45.08kg. A linear least squares polynomial was fit through the known loads versus measured loads. The differences between the measured forces and this fit would then show linearity. To exclude outliers, three times the standard deviation of these differences was taken as non-linearity measure instead of the maximum difference. Furthermore, a second order linear least squares polynomial was fit through the data. The fit was then evaluated by calculating R^2 for both the first and second order polynomial.

D.1.5. Delay

For the delay, it is important to know the difference between the first moment a force is applied and the first moment a force is measured. To measure this, a hammer with a marker on it was used. Both belts were hit with the hammer for fifteen times. The first moment at which the marker was at it lowest vertical position was taken as the first instance on which the hammer hit the force plate. The moment at which the measured force first exceeded five times the standard deviation above or below the baseline was used as the moment on which force was measured. No filter was used for this data.

D.2. Data analysis

Differences in accuracy between groups (e.g. different speeds, different AP positions et cetera) have been studied using a three way analysis of variance in Matlab (ANOVAN) with a 5% confidence level ($\alpha = 0.05$). A multiple comparison test using the Bonferroni method was used to find out which groups were different. All data was low-pass filtered at 20Hz with a second order Butterworth filter and using zero-phase digital filtering.

For the constant trials, high accelerations were present just before and after changing direction of movement. Because of this only the middlemost 50% of the treadmill of these trials is used. This means that for every constant trial only the data was used where the marker position in z-direction is between -0.57m and 0.21m.

D.3. Optimal calibration trial

D.3.1. Equipment

As for experiment one, a GRAIL system (Motekforce Link) with a split belt instrumented treadmill was used. The system was equipped with actuators capable of translation in the mediolateral direction (sway) and rotation for sagittal pitch. Both belt assemblies have a weight of 150kgs, which is located between the force sensors and the belt. The accelerometers that were used were two triaxial accelerometers (4030 2G range, Measurement Specialties). One was attached to the posterior left and the other to the anterior right. The set up can be seen in Figure D.5.

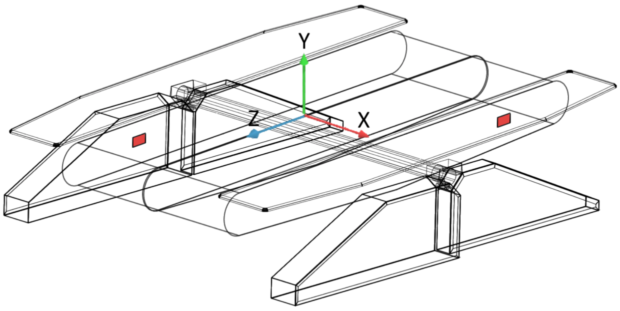

Figure D.5: Treadmill set up with the accelerometers in red and the coordinate system x-y-z [17].

All data was obtained from Vicon. This included the accelerometer data (1000Hz), the force plate data (1000Hz) and the belt speed (200Hz) which was obtained by streaming the belt speed from D-Flow to Vicon. For the validation trials only the data of the left force plate was used. The hand rails were left on the treadmill as this usually done when using perturbations.

D.3.2. Interaction between models

Two inertia compensation methods were used, one for pitch and sway and one for belt perturbations. Therefore, it was checked whether no interaction occurred between pitch and sway movement and belt accelerations. This was checked by recording accelerometer data while giving belt perturbations.

D.3.3. Pitch and Sway

The methods for pitch and sway perturbations were according to the paper of Hnat (2018) [17]. In order to find out what the best calibration trial is for the inertia compensation, several calibration trials had to be developed. A calibration trial consisted of several perturbations of an empty treadmill. The forces measured by the force plate and the accelerations measured by the accelerometers were then used to base an inertia compensation matrix on. This was done in Matlab using the backslash operator:

$$C = A_{calibrationtrial} \backslash F_{calibrationtrial} \tag{D.4}$$

Where A is the matrix with measured accelerometer data, F the matrix with the forces as measured by the force plate and C the inertia compensation matrix.

This would lead to one compensation matrix for each calibration trial. A second type of trial, the validation trial, was then used to test every compensation matrix on. During this trial, force measurements were captured and forces were predicted using the compensation matrix and accelerometer data.

$$\hat{F} = A_{valtrial} * C \tag{D.5}$$

Where A is the matrix with measured accelerometer data from the validation trial, C the inertia compensation matrix from the calibration trial and F the estimated forces.

The difference between the predicted forces and measured forces was seen as the error. The smaller this difference, the better the inertia compensation and thus the better the calibration trial.

This was calculated as following:

$$RMSE = \sqrt{\frac{\sum(\hat{F} - F_{valtrial})^2}{n}} \tag{D.6}$$

Where n is the number of samples, $\hat{F}$ the forces as calculated by Equation D.5 and $F_{valtrial}$ the measured forces in the validation trial.

D.3.4. Belt accelerations

For the belt accelerations, the methods were similar to the paper of Hnat et al. (2014) [18]. The belt perturbations cause an artefact in the measurement of the pitching moment because of the torque which the motor generates during acceleration and deceleration. This method uses a linear second-order discrete time model was used to predict the forces based on the belt speed. The belt speed was obtained at 200Hz, whereas the forces were obtained at 1000Hz. The output of the belt speed was, however, given in 1000Hz. One would expect a discrete, stagewise signal but this was not the case due to some noise. To obtain a smooth belt speed, a cubic spline smoothing method could be a useful method. However, this is not available in D-Flow and can therefore not be used in further projects. Spline smoothing methods use polynomials to obtain the optimal goodness of fit using a smoothing parameter [19]. This smoothing parameter can be used to calculate the optimal cut-off frequency which can be used in D-Flow. It does so by minimizing the following equation:

$$\sum_{i=1}^{N}(f(t_i) - x_i)^2 + p\int f^{(\frac{n+1}{2})}(t)^2 dt \tag{D.7}$$

In which $f(t)$ is a function that best fits the data, t and x are data samples, n is the order of the spline method and p is the smoothing parameter. The data samples in x consist of noisy data. For this study, a cubic spline smoothing method (CSAPS-function Matlab) was used which makes use of a second derivative as it is a third degree method. The smoothing parameter obtained from this was then used to calculated the optimal cut-off frequency for this filter:

$$wo = (p * T)^{(-0.5/M)} \tag{D.8}$$

With wo the cutoff frequency, p the smoothing parameter, T the sampling interval, and $2M$ the order of the spline [20]. This resulted in a 10Hz cut-off frequency which was used for both the belt speed and the pitching moment. With a typical cut-off frequency of 6Hz for gait analysis, 10 Hz seems appropriate for a little higher frequency movements like during perturbations. The 10Hz cut-off frequency can be set in D-Flow for following studies that use the inertia compensation model. The belt velocity and pitch moment were filtered using this cut-off frequency and downsampled to 100Hz, just like D-Flow normally does.

The belt speed was derived with the use of a central difference formula using gradient in Matlab. In Matlab, fmincon was used to minimize the sum of the squared error between the estimated forces and measured forces. Using the model, the forces and moments could be calculated for following trials. Again, the difference between the predicted forces and measured forces was seen as the error. The smaller this difference, the better the inertia compensation and thus the calibration trial.

$$RMSE = \sqrt{\frac{\sum(F_{estimate} - F_{valtrial})^2}{n}} \tag{D.9}$$

Where n is the number of samples, $F_{estimate}$ the forces as calculated by D.5 and $F_{valtrial}$ the measured forces in the validation trial.

D.3.5. Signals

All input signals for the treadmill can be found in Appendix E.

D.4. Data analysis

A ranking was made based on the percentage of root mean square error (RMSE) reduction in order to be able to choose the best calibration trial. All calibration trials were ranked for each combination of the four validation trials and six forces and moments. An overall ranking was made for each calibration trial using the average of the 24 rankings. For each combination of a validation trial and a force, the best calibration trial was chosen, all based on percentage of RMSE reduction. The calibration trial that ended up most in both the ranking and the best trial table was chosen as the best calibration trial. The two different speeds and two different durations were compared as well. This was done for the best trial with the help of a n-way analysis of variance in Matlab (ANOVAN). A multiple comparison test using a Bonferroni correction was used to find out what the differences between the groups were.

D.5. Effect of inertia compensation on a musculoskeletal model

D.5.1. Equipment

The same set-up as for experiment 2 was used. This time the data was recorded and processed with, respectively, D-Flow software version 3.30 and 3.32 Beta 11 (Motekforce Link) with a custom option to replay a C3D-file. A safety harness for the subjects was added and attached to the ceiling. The hand rails were left on the treadmill as this usually done in other use. Subjects were provided with 46 markers as specified for the musculoskeletal model (Human Body Model, Motekforce Link) [9]. A motion capture system of Vicon was used with 10 infra-red motion capture cameras connected to Nexus 2.6 (Vicon software).

D.5.2. Experimental design

Only the pitch and sway inertia compensation method was evaluated as the one for belt perturbations was not yet implemented in the D-Flow software. The experiment consisted of a calibration trial, a familiarization trial and three trials with different conditions. Subjects were instructed to walk like they normally would. Each trial started with a subject standing still with their arms spread (T-pose). This was needed to allow accurate calibration during the reprocessing of each file. All trials were run at an average walking speed for young healthy adults of 1.3m/s (4.7km/h) [21].

- **Calibration trial.** The calibration trial consisted of a few seconds in T-pose with a consecutive 5 steps of walking.
- **Familiarization trial.** The familiarization trial included six minutes of walking on the treadmill.
- **Baseline measurement.** Two minutes of normal walking without any perturbations.
- **Sway perturbations.** About twelve minutes of walking with 20 contralateral sway perturbations at initial contact. This meant that the treadmill moved to the left at right initial contact and thereby caused lateral balance loss. Recovery from this includes a narrow or even a cross-over step. This type of perturbation was chosen over a ipsilateral sway perturbation because a contralateral perturbation is seen as most difficult. During a perturbation the entire platform was moved 5cm with a speed of 0.30m/s. The platform was slowly returned to base after seven seconds. Time between perturbations was chosen randomly, the same for all subjects however, between 10 and 60 seconds. Perturbations were randomly divided over the left and right foot.
- **Pitching.** Two minutes of up and downhill walking (a sinusoidal signal from -10° to 10° of pitch with a wavelength of 30s).

The measures used were the kinetic residuals of the Human Body Model [9]. The Human Body Model combines the motion capture and force plate data for inverse kinematics and inverse dynamics. The forces that cannot be prescribed to any joint are called the residual forces and are prescribed to the pelvis. Those kinetic residuals can be seen as the experimental and modeling error and are therefore a good measure of the musculoskeletal model accuracy.

D.5.3. D-Flow application

The D-Flow application was mainly build up of building blocks from the D-Flow toolbox. The used building blocks were:

- Forest environment
- Count down
- Gait event detection
- V-Gait perturbations
- Trigger perturbation

Added to this were a phidget with corresponding scripts to allow a Vicon connection, a treadmill and Mocap module and timers. The timers fired events to start and stop the different trials. A built-in step detection algorithm was used to provide information on initial contact which was needed to initiate perturbations. The coordinate-based algorithm was used which is based on the method described in the paper of Zeni et al. (2008)[22]. The timing between perturbations was set manually. The time between perturbations for all 20 perturbations was: [17, 58, 37, 17, 23, 52, 22, 51, 22, 57, 27, 20, 22, 41, 34, 27, 52, 39, 38, 56]. A forest environment with moving path and ground projection was used during all trials.

D.5.4. Subjects

A total of 10 young healthy adults participated in the experiment. Only data of 9 subjects (mean age 26 (± 3.8) years) could be used due to poor marker data of one of the subjects. All participants were between 18 and 35 years old without any neurological or orthopedic conditions that could influence balance or walking. Six males and three females participated (mean length 1.78m (± 0.13m), mean weight 74.6 kg (± 11.45kg)) and were all wearing their own sneakers. All participants gave their informed consent. The study was approved by the Human Research Ethics Committee of the TU Delft.

D.5.5. Data processing

All data was captured in Vicon Nexus 2.7. This included marker data (100 Hz), analog data from the force plates (1000 Hz), accelerometer data (1000 Hz), the belt speed (200 Hz) and the initial moments of the perturbations. The latter two of which were streamed from D-Flow to Vicon. It was then processed in Nexus using 'Reconstruct - Label - Fill Gaps Woltring - Delete unlabeled trajectories - Functional skeleton calibration - Save Trial - C3D + VSK - Export ASCII'. Unfilled gaps were filled using cyclic or rigid body fill before deleting unlabeled trajectories.

Every trial was then reprocessed in D-Flow to obtain HBM and gait data. A custom version of D-Flow 3.32.0 Beta 11 was then used that enabled playback of a C3D file. The weight of each subject was calculated manually using Matlab and filled in the Mocap module. For the baseline measurements the file was played back on a normal computer while recording HBM and gait data. For the sway perturbation and pitching measurements the file was played back on a computer connected to the GRAIL simultaneously with the script that initiated perturbations. In this way D-Flow received data about platform translations and could compensate for this when calculating kinetics. It was, however, seen that a maximal differences in outcomes of the GRAIL movement of two frames was found between different playback trials. On top of this, there is still a delay of 3 frames (0.03s) between the processing of the motion capture data and the processing of the platform position. Artificially compensating for this delay resulted in differences in average kinetic residuals of maximal 0.5N. Due to the small differences no artificial compensation for the delay was used in this study but more research on this could improve the results. The cut-off frequency for the HBM was set to 6 Hz which is similar to experiment 2 and literature.

In first instance, it was noticed that HBM could not find a solution for about a hundred out of a full trial of 12000 frames. A faster computer was used to solve this. Also, the maximum time used for the kinetic solver was increased from 0.002s to 0.008s. All other computer settings were optimized to maximize performance. The final results only showed this problem for a maximum of 4 frames out of an entire trial.

D.5.6. Data analysis

The inertia compensation model was trained on the best trial obtained from the second experiment (a random signal with a square wave of sway). The forces were then corrected before they were fed into the Human Body Model as described in Appendix C.

The weight of the subject was obtained by force plate data of the first 100 frames of a trial with a person in T-pose.

Data of the baseline, sway and pitch trials were used. For the baseline and pitch trials a total of 100 steps per subject were used. For the sway trial only data during a perturbation was used to do the calculations with. A perturbation was started at initial contact. The perturbation started at approximately 10 per cent of the gait cycle. The moment a perturbation started was recorded by sending a pulse from D-Flow to Vicon at the moment a perturbation was sent to the VGait module. Some of these pulses could not be detected after reprocessing in D-Flow due to downsampling. Therefore the raw 1000Hz data from Vicon was used to calculate initiation of the perturbation.

All data was normalized to a gait cycle to show effects on the kinetic residuals in the different parts of the gait cycle. A Matlab-file ('normalizetimebase.m') from Jaap Harlaar was used as a basis to normalize the data. There were around 90 frames per gait cycle which were then normalized to a 101 samples so the amount of samples stayed quite much the same. This resulted in 50 normalized gait cycles for the pitch and baseline measurement per subject and for 20 cycles for the sway trial. The average of these trials was calculated per subject using the RMS. This average was used to calculate the overall average.

D.5.7. Statistical analysis

The entire statistical analysis was performed in SPSS 25.0. A 2(IC) x 3(conditions) repeated measures two-way ANOVA ($\alpha = 0.05$) was performed. A paired samples t-test was performed for comparison for each condition with and without IC. Also, sway with IC and pitch with IC were compared to baseline without IC. A Bonferroni correction was used for these five multiple comparisons. The Friedman's test was used as a non-parametric equivalent for the repeated measures two-way ANOVA. A Wilcoxon signed rank test was used in the same way as the paired samples t-test for the parametric method. The same Bonferroni correction was used for the non-parametric test.

E

Signals optimal calibration trial

Two different types of signals were used to find the best calibration trial. First of all the signals for the calibration trials, on which the inertia compensation was based. The others signals were meant for the validation trials, on which the inertia compensation was tested. All of the signals were made in Python and uploaded to D-Flow 3.28.

E.1. Calibration trials

Two types of calibration trials were made, one for pitch and sway and one for belt accelerations. Those were based on experiences and ideas from earlier trials when testing the inertia compensation. The following signals were made for the pitch and sway perturbations:

- Random signal for 60 seconds
- Random signal for 300 seconds
- Random signal (60s) + 3 times a square wave of maximum sway perturbations (5 to -5 cm)
- Random signal (300s) with 3 times a square wave of maximum sway perturbations in it (5 to -5 cm)
- Random signal (60s) with 3 times a gap in which no perturbations occurred in it
- Random signal (300s) with 15 times a gap in which no perturbations occurred in it
- Random signal (60s) + 3 times a square wave of maximum pitch perturbations (10 to -10 degrees)
- Random signal (300s) with 3 times a square wave of maximum pitch perturbations in it (10 to -10 degrees)
- Random signal (60s) + 3 times a constant sway (5cm and 2.5cm)
- Random signal (300s) with 3 times a constant sway in it (5cm and 2.5cm)
- Random signal (60s) + 3 times a constant pitch (10 degrees and 5 degrees)
- Random signal (300s) with 3 times a constant pitch in it (10 degrees and 5 degrees)
- Random signal (60s) + all of the above (square wave pitch & sway, constant pitch & sway, gaps)
- Random signal (300s) with all of the above in it (square wave pitch & sway, constant pitch & sway, gaps)

All of the above signals can be found visually in Section E.4. The random signal was based on the article by Hnat et al. (2018) [17] and Python files by Lars Aartsen. The maximum possible position amplitudes for pitch and sway are 10 degrees and 5cm, respectively. In the signals, 95% of this was used to prevent it from reaching the end entirely. All of this was done with a belt running at 3 m/s and with the motor running but at 0 m/s belt speed. The random signal was a Gaussian white noise with zero mean and standard deviations of $0.707 m/s^2$ and $127 deg/s^2$ for sway and pitch, respectively. The signal was integrated twice to obtain accelerations that were achievable and a bidirectional Butterworth filter was used.

The signals as mentioned below were made for belt acceleration perturbations.

- Random signal for 60 seconds
- Random signal for 300 seconds
- Random signal (60s) with 3 times a gap in which no perturbations occurred
- Random signal (300s) with 15 times a gap in which no perturbations occurred
- Random signal (60s) + 3 times a square wave of maximum acceleration (from 3 to -3 m/s)
- Random signal (300s) with 3 times a square wave of maximum acceleration in it (from 3 to -3 m/s)
- Random signal (60s) + 3 times a constant speed (-1 m/s and -0.3 m/s)
- Random signal (300s) with 3 times a constant speed in it (-1 m/s and -0.3 m/s)
- Random signal (60s) + all of the above (square wave acceleration, constant speed, gaps)
- Random signal (300s) with all of the above (square wave acceleration, constant speed, gaps) in it

The random signal for the belt acceleration trials was based on the article by Hnat & Van den Bogert (2014) [18] and Python files by Lars Aartsen. All signals were run with a mean speed of 1.0m/s (with a variance in acceleration of $25 m/s^2$) and 2.0m/s (with a variance in acceleration of $2000 m/s^2$). A white noise signal was used with accelerations between -15 m/s and 15 m/s. Again, 95% of this was used to prevent it from reaching the high accelerations. The signal was integrated once to obtain belt speed.

E.2. Validation trials

Four different trials were used for validation of the inertia compensation model. The validation trials are representative of the normal use and involve different ways of walking and different perturbations. In the first trial, a subject walked on the right belt (belt speed 1.3m/s) while being perturbed with sway movements (0.31m/s and an amplitude of -/+0.05m). The second validation trial used pitching movements in a similar way as they are used in the real world. This trial involved a subject walking on the right belt (belt speed 1.3m/s) while the treadmill was pitching. The pitch varied between minus and plus 10 degrees with a sinusoidal movement with a wavelength of 30 seconds. For the third trial, a subject ran on the right belt with a belt speed of 2.5m/s (9km/h). The fourth trial had someone standing and moving on the boarding to simulate forces as exerted by subjects while walking or running but without having anyone on the belts. These trials were used as a validation for the pitch and sway inertia compensation.

The fourth trial was used for the validation of the inertia compensation model for the belt acceleration. This included a trial with belt accelerations and decelerations similar to normal use. The belt accelerations had a duration of 0.15s, an intensity of $12 m/s^2$ and were given every five seconds.

E.3. Calibration trials pitch and sway

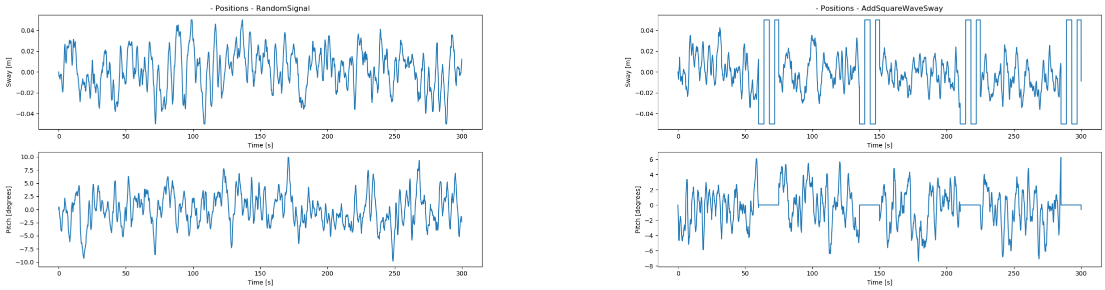

(a) Random Signal.

(b) Random Signal with a square wave of sway in it.

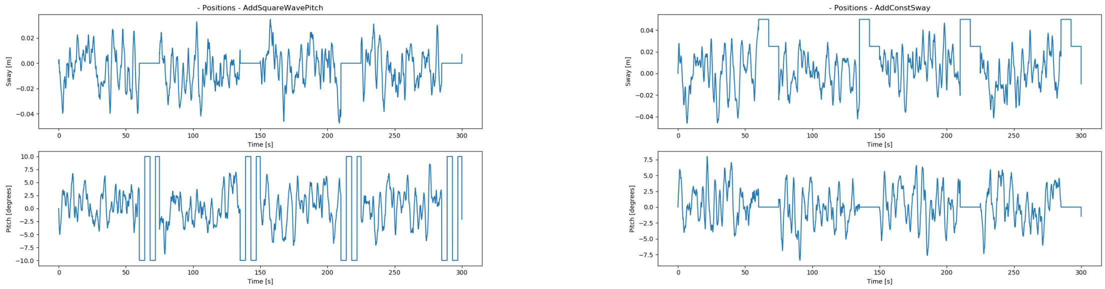

(c) Random Signal with a square wave of pitch in it.

(d) Random Signal with a constant part of sway in it.

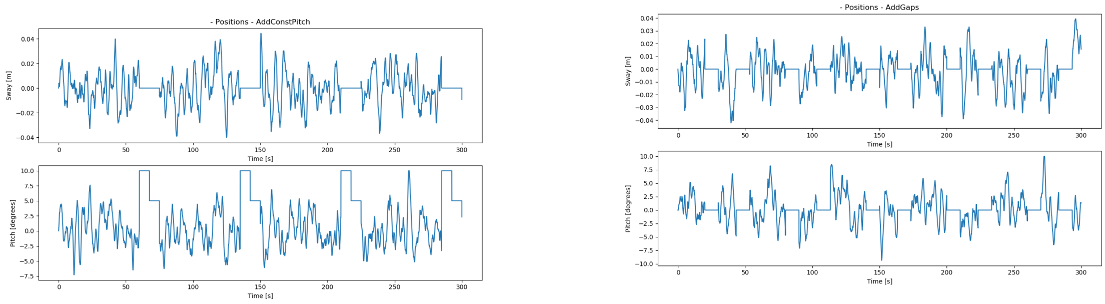

(e) Random Signal with a constant part of pitch in it.

(f) Random Signal with some gaps in which nothing happens in it.

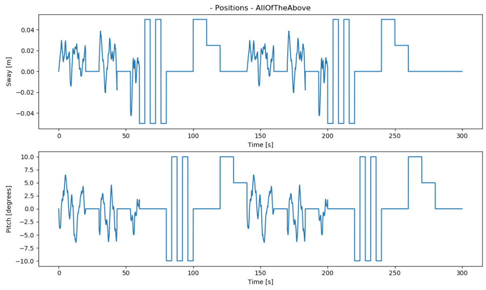

(g) Random Signal with a square wave of sway, a square wave of pitch, a constant part of sway, a constant part of pitch and gaps in it.

Figure E.1: All calibration trial signals for pitch and sway perturbation of 300 seconds.

E.4. Calibration trials belt acceleration

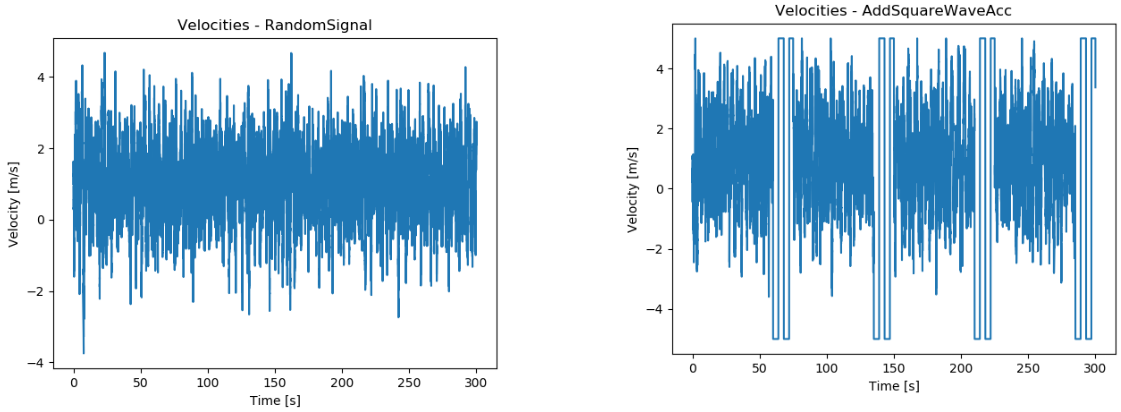

(a) Random Signal.

(b) Random Signal with a square wave of acceleration in it.

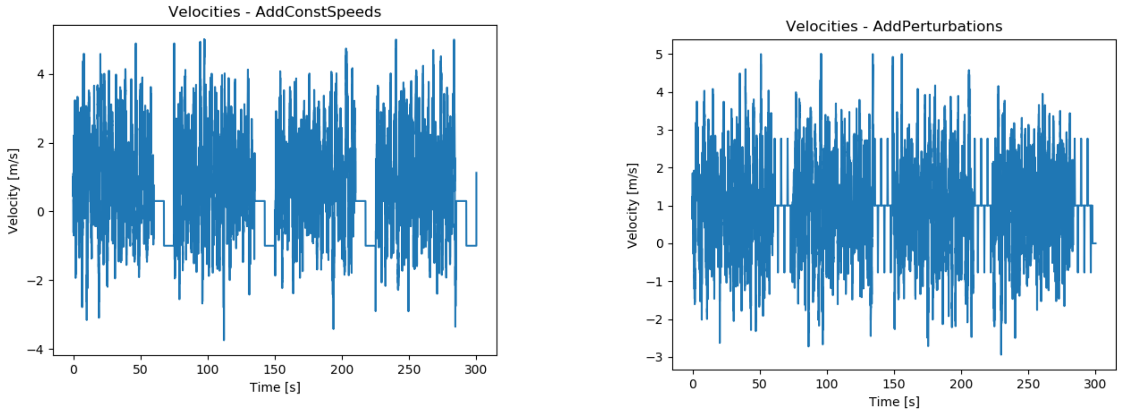

(c) Random Signal with parts with constant speeds in it.

(d) Random Signal with belt perturbations in it.

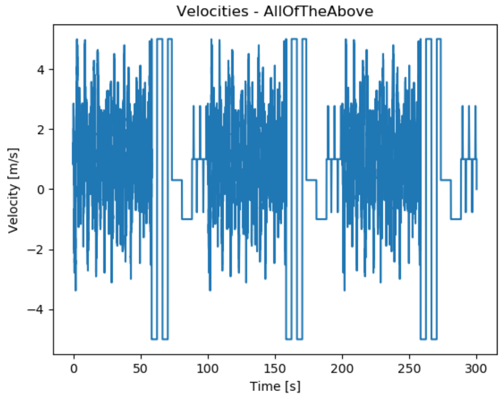

(e) Random Signal with a square wave of acceleration, a constant speed part of sway and perturbations in it.

Figure E.2: All calibration trial signals for belt acceleration of 300 seconds.

F

Experiment results

F.1. Dynamic validation results

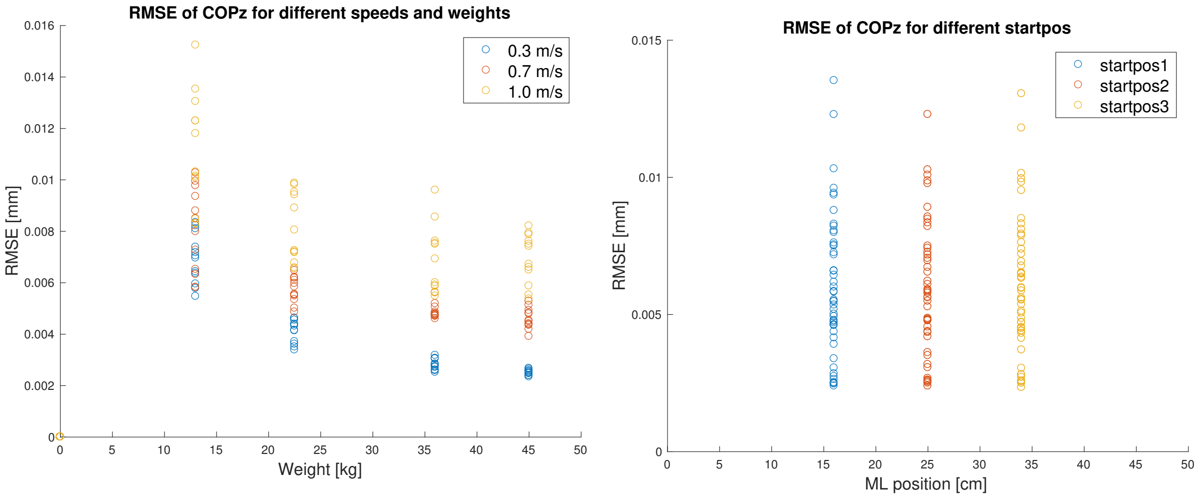

(a) RMSE for different anterior posterior positions and speeds.

(b) RMSE for all trials for different ML positions.

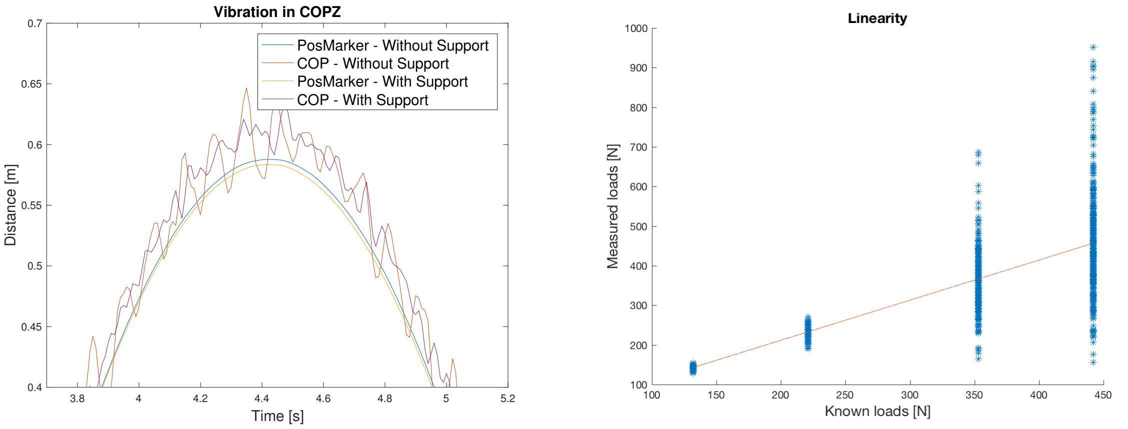

(c) Vibration in COPZ and marker position with and without metal supports.

(d) Linearity of the force plate in vertical force measurement.

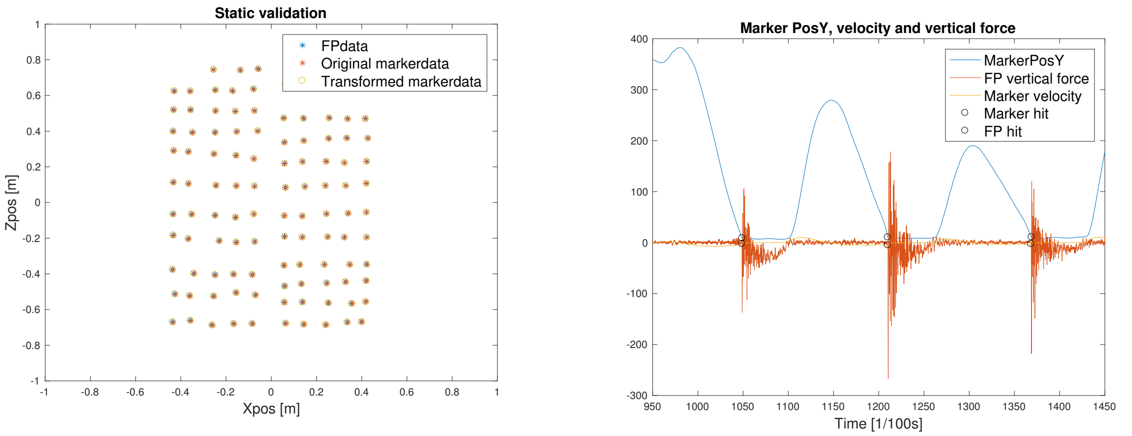

(e) Static validation data before and after the transformation.

(f) Delay between the marker data and force plate data.

Figure F.1: Results of the dynamic validation experiments.

F.2. Optimal calibration trial results

F.2.1. Interaction between models

The accelerometer data while perturbing by belt accelerations can be seen in Figure F.2. No reaction can be seen in the accelerometer during the accelerations.

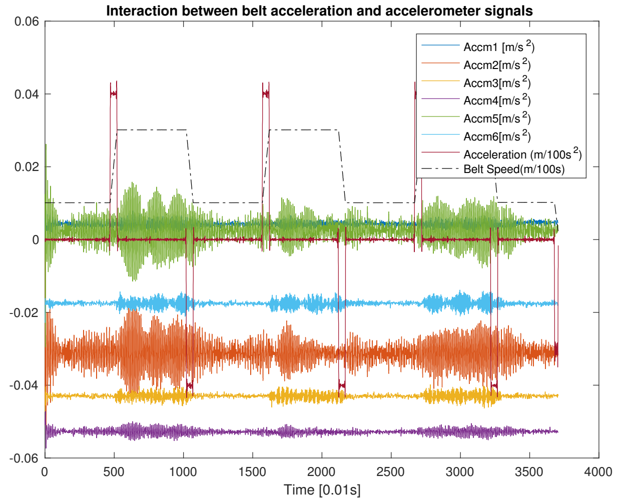

Figure F.2: Data of six accelerometers that were attached to the treadmill while giving belt perturbations. No increase of the accelerometer signals can be seen during acceleration.

F.2.2. Plots for all validation trials

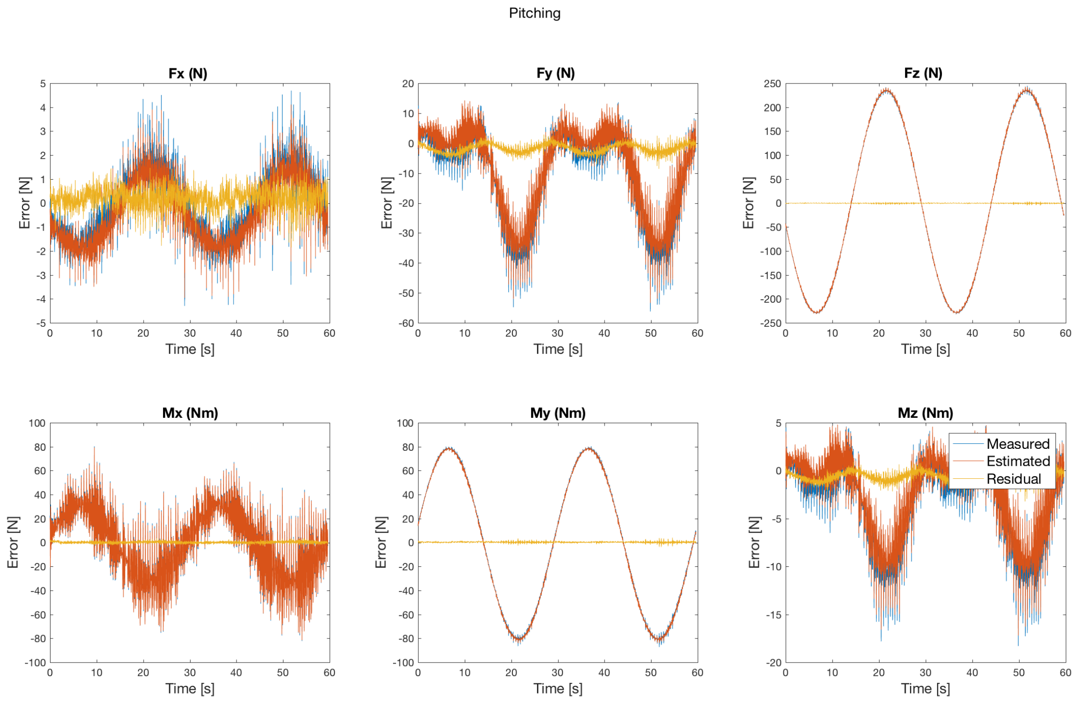

Figure F.3: Forces and moments with the best calibration trial for the pitching validation trial.

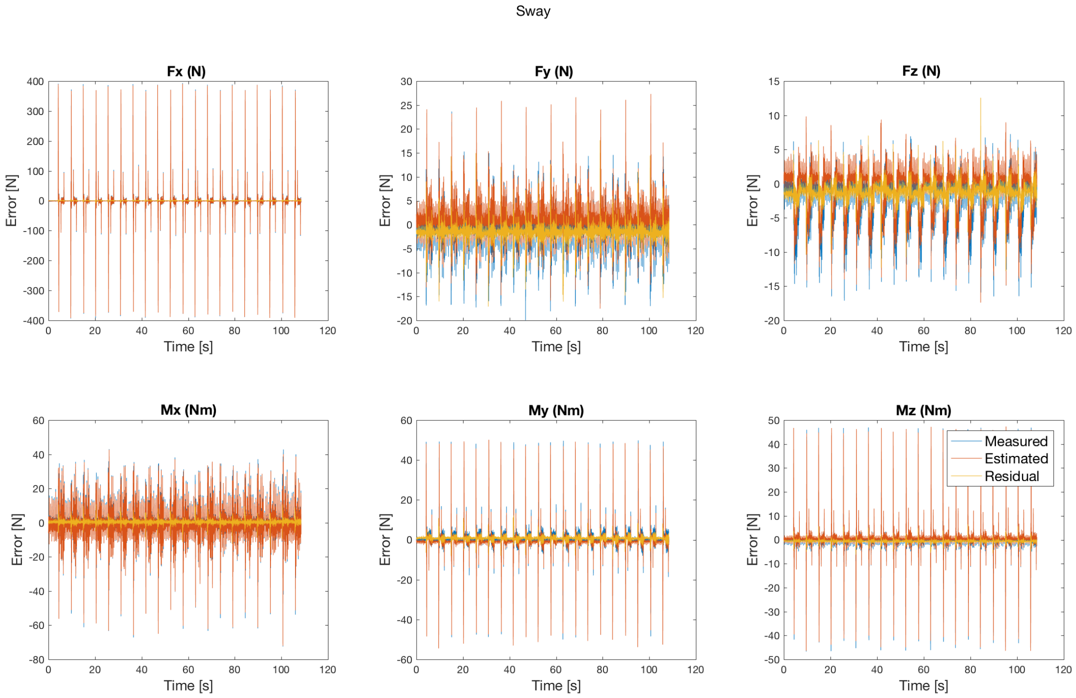

Figure F.4: Forces and moments with the best calibration trial for the sway validation trial.

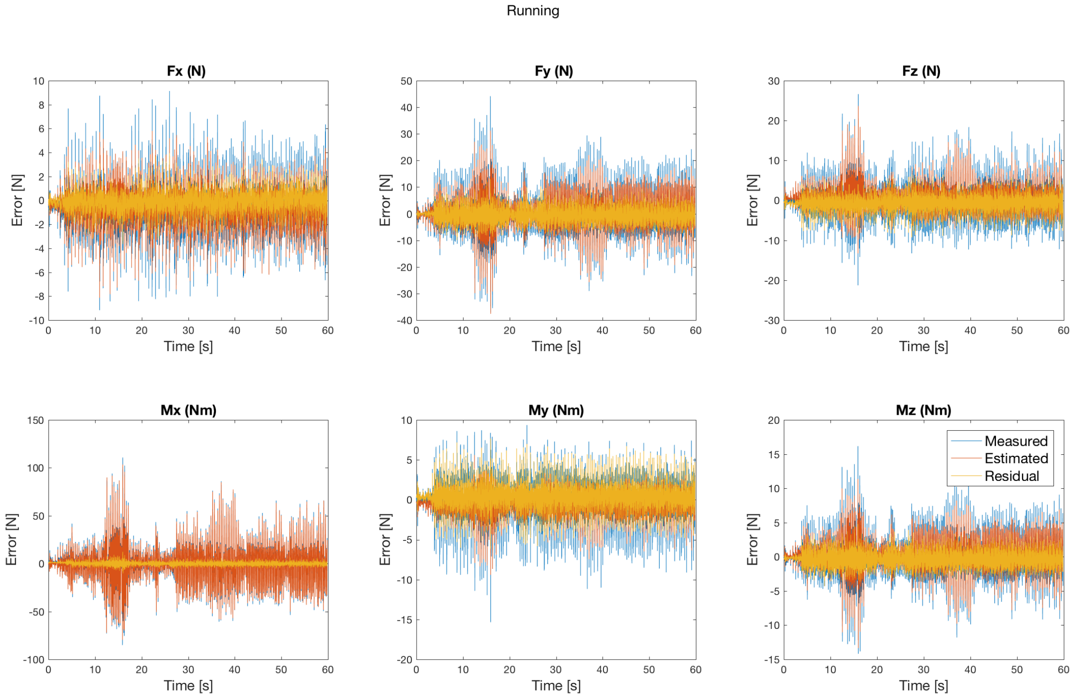

Figure F.5: Forces and moments with the best calibration trial for the running validation trial.

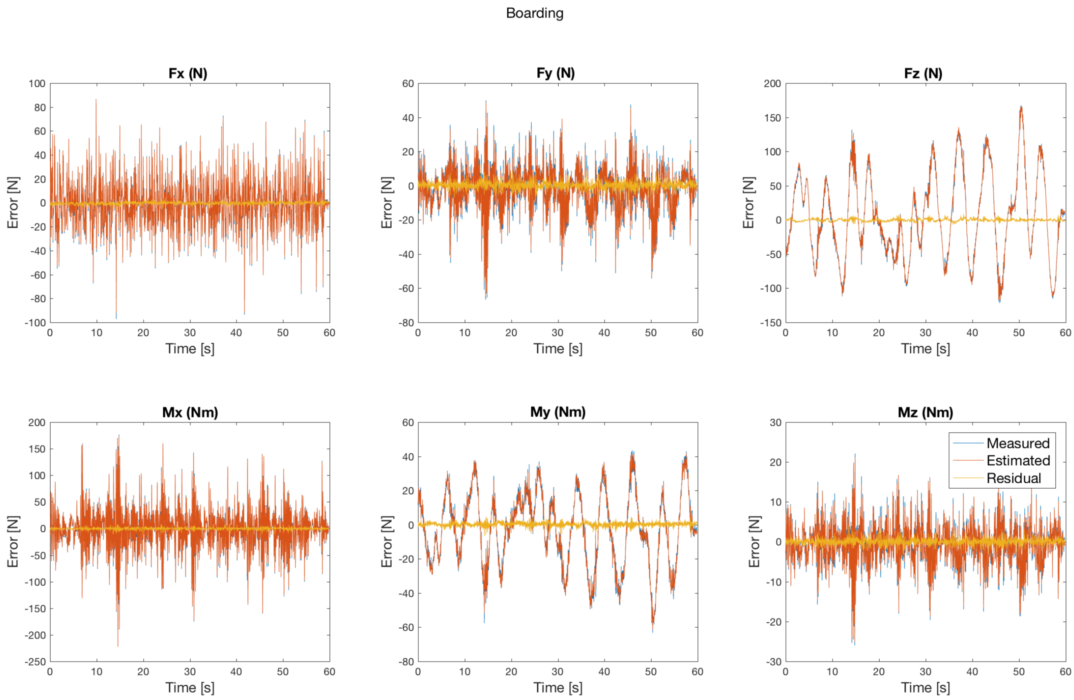

Figure F.6: Forces and moments with the best calibration trial for the boarding validation trial.

F.2.3. Best calibration trial pitch and sway

The table with the best calibration trial for each combination of validation trial and force or moment can be seen in Figure F.7. It can be seen that the square wave sway calibration trial appeared in the table for eight times, whereas the calibration trial with gaps only appeared three times. The calibration trial with all of the variations turned up seven times.

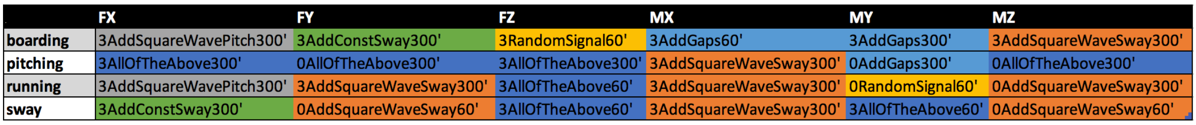

	FX	FY	FZ	MX	MY	MZ
boarding	3AddSquareWavePitch300'	3AddConstSway300'	3RandomSignal60'	3AddGaps60'	3AddGaps300'	3AddSquareWaveSway300'
pitching	3AllOfTheAbove300'	0AllOfTheAbove300'	3AllOfTheAbove300'	3AddSquareWaveSway300'	0AddGaps300'	0AllOfTheAbove300'
running	3AddSquareWavePitch300'	3AddSquareWaveSway300'	3AllOfTheAbove60'	3AddSquareWaveSway300'	0RandomSignal60'	0AddSquareWaveSway300'
sway	3AddConstSway300'	0AddSquareWaveSway60'	3AllOfTheAbove60'	3AddSquareWaveSway300'	3AllOfTheAbove60'	0AddSquareWaveSway60'

Figure F.7: Table showing the best calibration trial for each combination of a validation trial and force or moment. The 0 or 3 in front of the name indicates a speed of 0 or 3 m/s. The 300 or 60 at the end of the name of a trial refer to the duration in seconds.

F.2.4. Speed and duration pitch and sway

Two different speeds and durations were examined to obtain the best calibration trial. It appeared that there was a significant difference for every force and moment. The best results can be seen in Table F.1. Looking at Figure F.7 with all best trials for each combination of validation trial and force, the speed of 3 m/s appears 17 times whereas 0 m/s only appears 7 times. The same table shows that a duration of 300 s is better than 60 s, with 16 and 8 occurrences, respectively.

Table F.1: Best speeds and durations for all forces and moments.

	Fx	**Fy**	**Fz**	**Mx**	**My**	**Mz**
Speed (m/s)	3	0	3	3	3	0
Time (s)	300	60	300	60	300	60

F.3. Evaluation of IC model results

F.3.1. Estimated marginal means for all measures

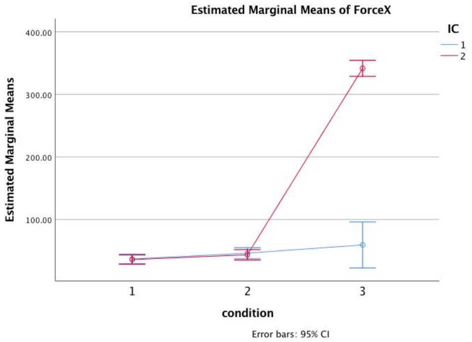

Figure F.8: Estimated marginal means for Force X. IC 1 = inertia compensation, IC 2 = no inertia compensation, Condition 1 = Baseline, Condition 2 = Sway, Condition 3 = Pitch. An interaction effect can be seen.

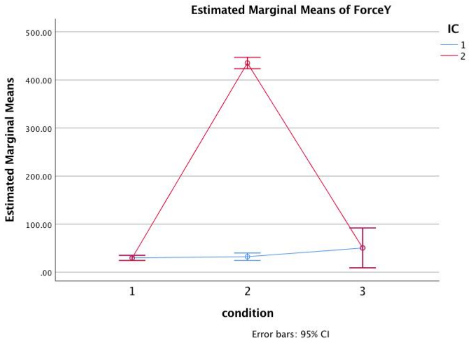

Figure F.9: Estimated marginal means for Force Y. IC 1 = inertia compensation, IC 2 = no inertia compensation, Condition 1 = Baseline, Condition 2 = Sway, Condition 3 = Pitch. An interaction effect can be seen.

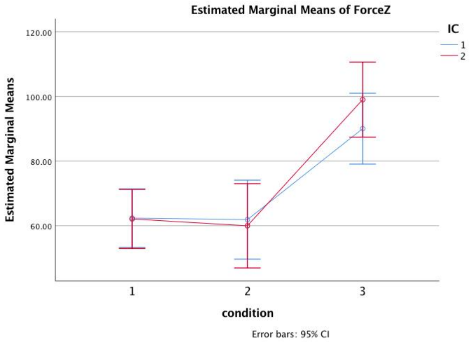

Figure F.10: Estimated marginal means for Force Z. IC 1 = inertia compensation, IC 2 = no inertia compensation, Condition 1 = Baseline, Condition 2 = Sway, Condition 3 = Pitch. An interaction effect can be seen.

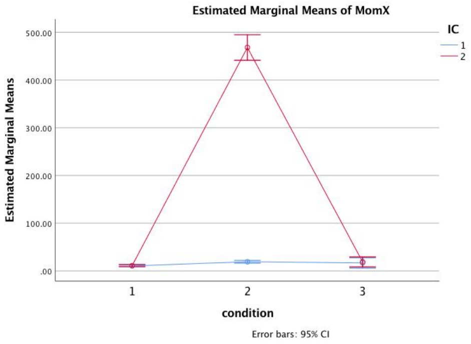

Figure F.11: Estimated marginal means for Moment X. IC 1 = inertia compensation, IC 2 = no inertia compensation, Condition 1 = Baseline, Condition 2 = Sway, Condition 3 = Pitch. An interaction effect can be seen.

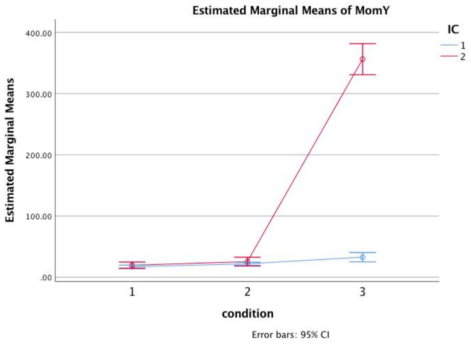

Figure F.12: Estimated marginal means for Moment Y. IC 1 = inertia compensation, IC 2 = no inertia compensation, Condition 1 = Baseline, Condition 2 = Sway, Condition 3 = Pitch. An interaction effect can be seen.

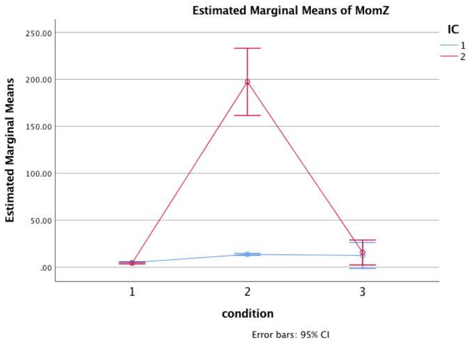

Figure F.13: Estimated marginal means for Moment Z. IC 1 = inertia compensation, IC 2 = no inertia compensation, Condition 1 = Baseline, Condition 2 = Sway, Condition 3 = Pitch. An interaction effect can be seen.

F.3.2. Raw data of the kinetic residuals of one subject

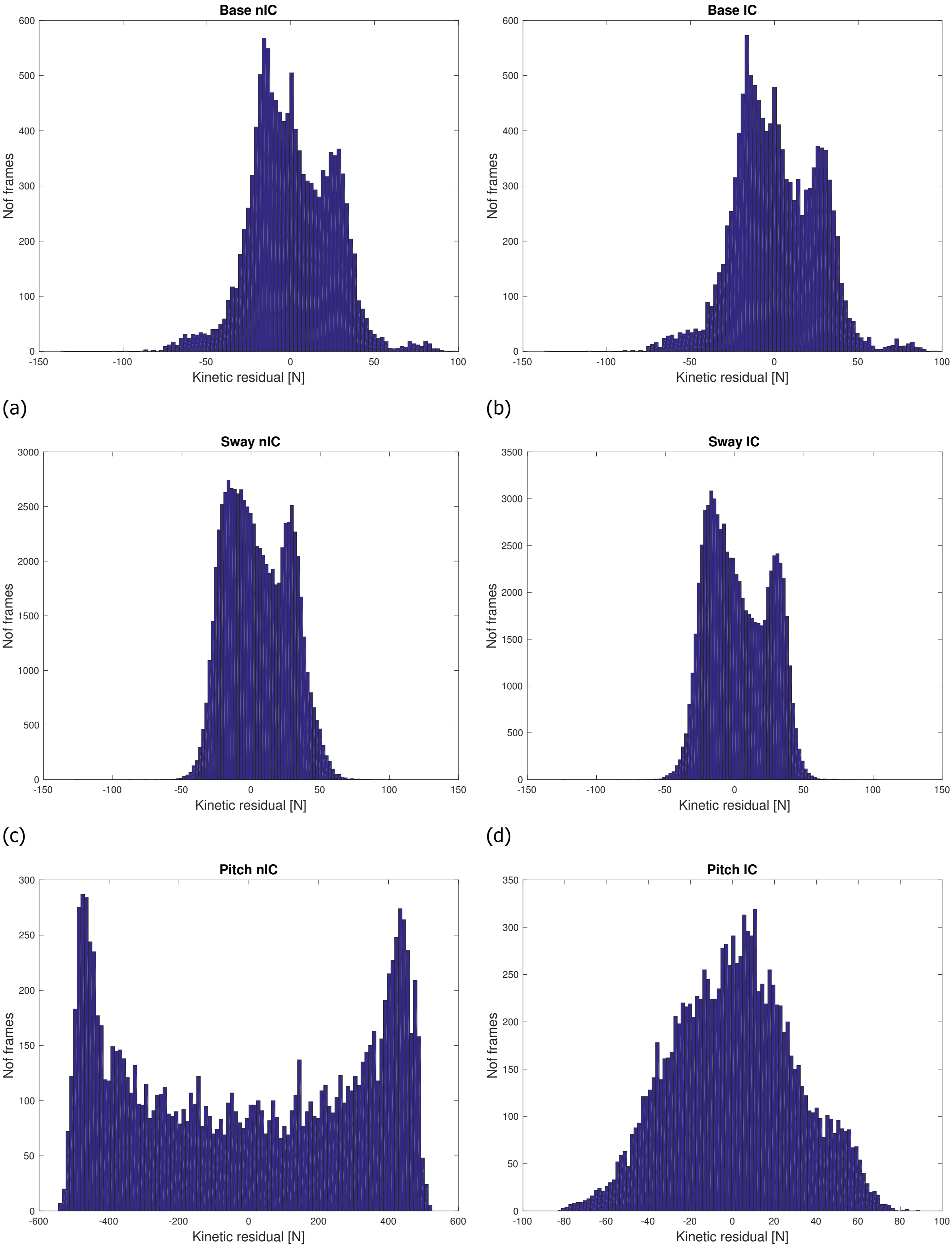

(a) (b)

(c) (d)

(e) (f)

Figure F.14: Raw data of the kinetic residuals of one subject for force X. The number of frames (nof frames) is shown for all conditions with IC (IC) and without IC (nIC).

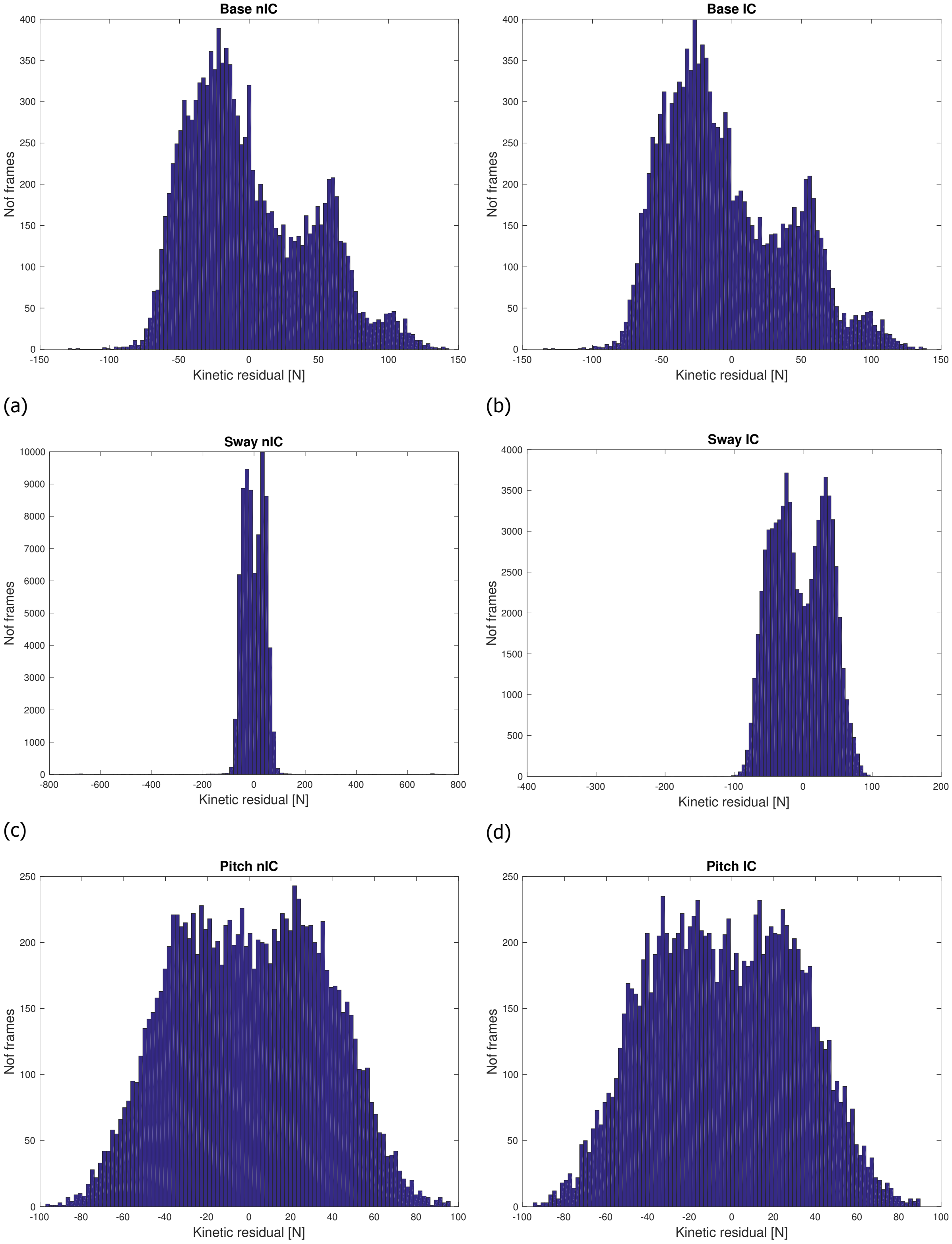

(a) (b)

(c) (d)

(e) (f)

Figure F.15: Raw data of the kinetic residuals of one subject for force Y. The number of frames (nof frames) is shown for all conditions with IC (IC) and without IC (nIC).

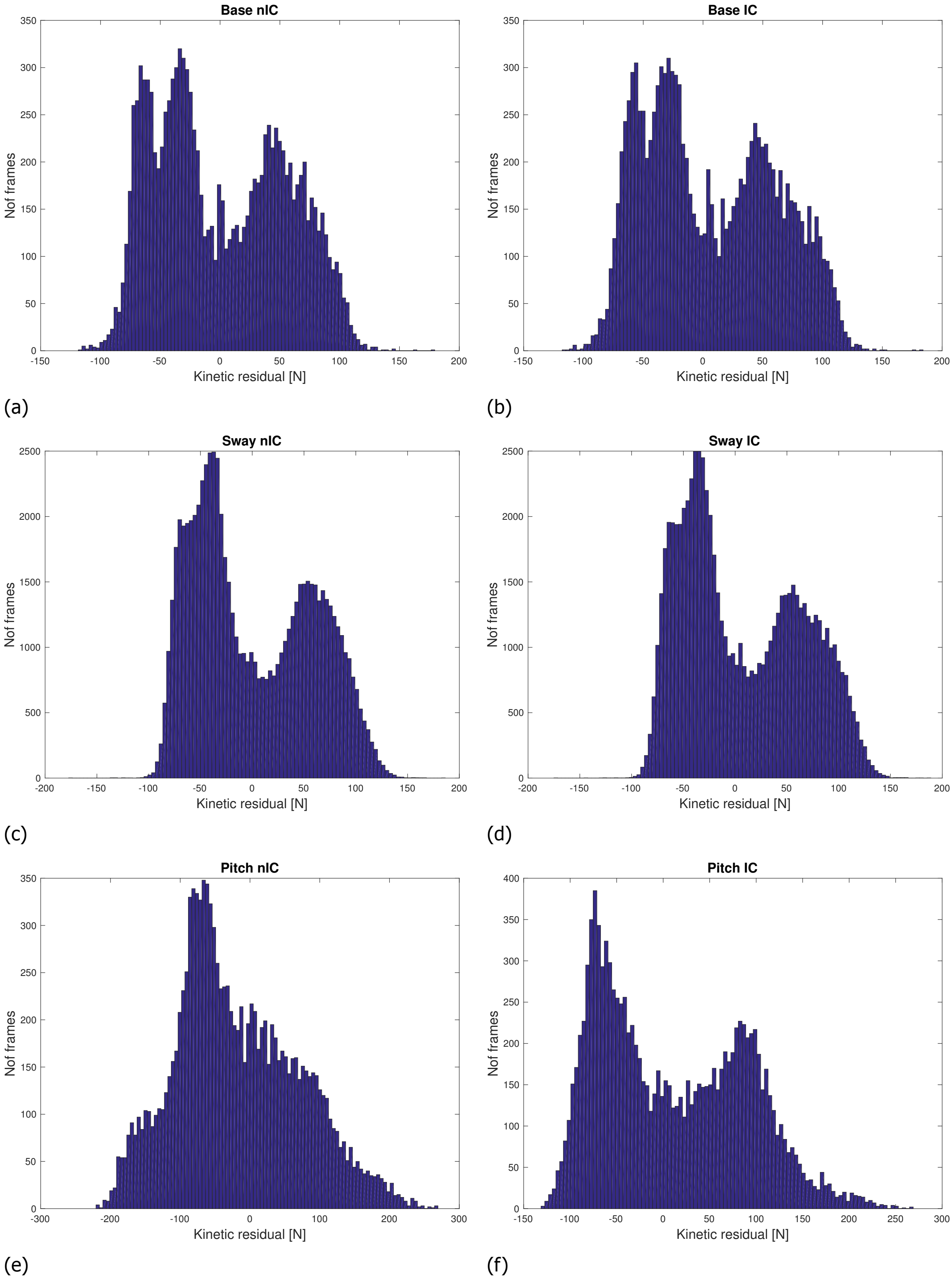

(a) (b) (c) (d) (e) (f)

Figure F.16: Raw data of the kinetic residuals of one subject for force Z. The number of frames (nof frames) is shown for all conditions with IC (IC) and without IC (nIC).

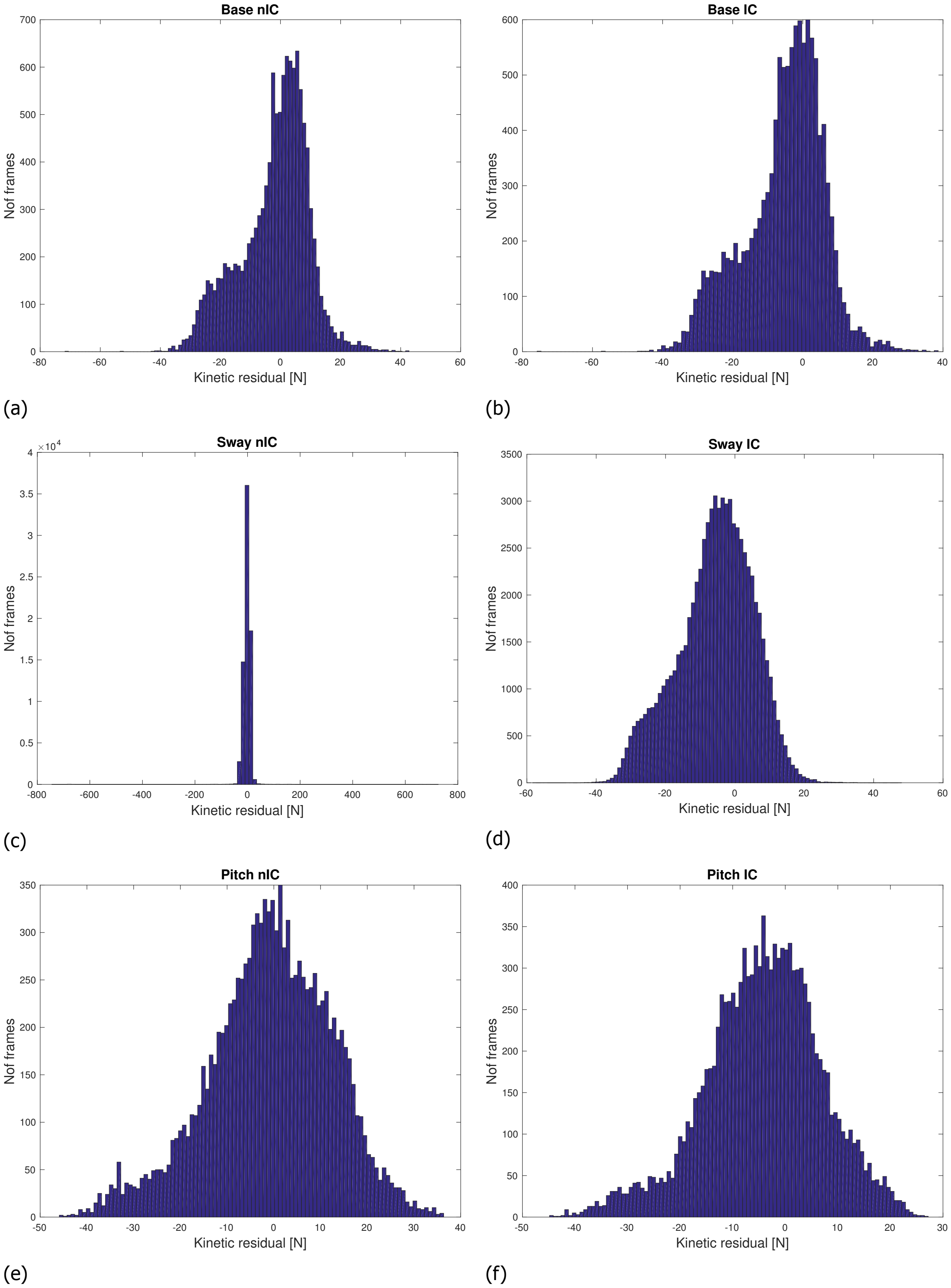

(a) (b)

(c) (d)

(e) (f)

Figure F.17: Raw data of the kinetic residuals of one subject for moment X. The number of frames (nof frames) is shown for all conditions with IC (IC) and without IC (nIC).

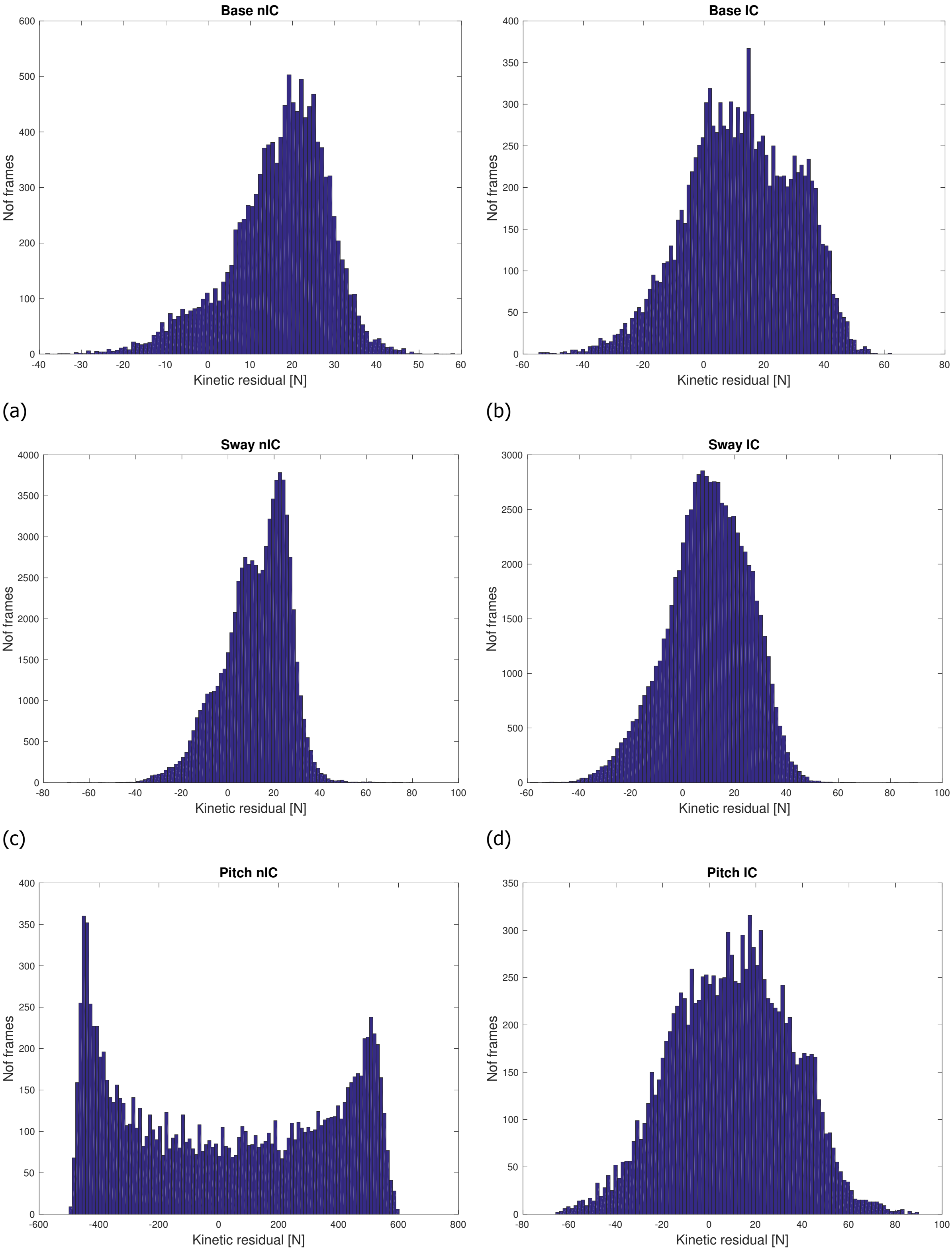

(a)

(b)

(c)

(d)

(e)

(f)

Figure F.18: Raw data of the kinetic residuals of one subject for moment Y. The number of frames (nof frames) is shown for all conditions with IC (IC) and without IC (nIC).

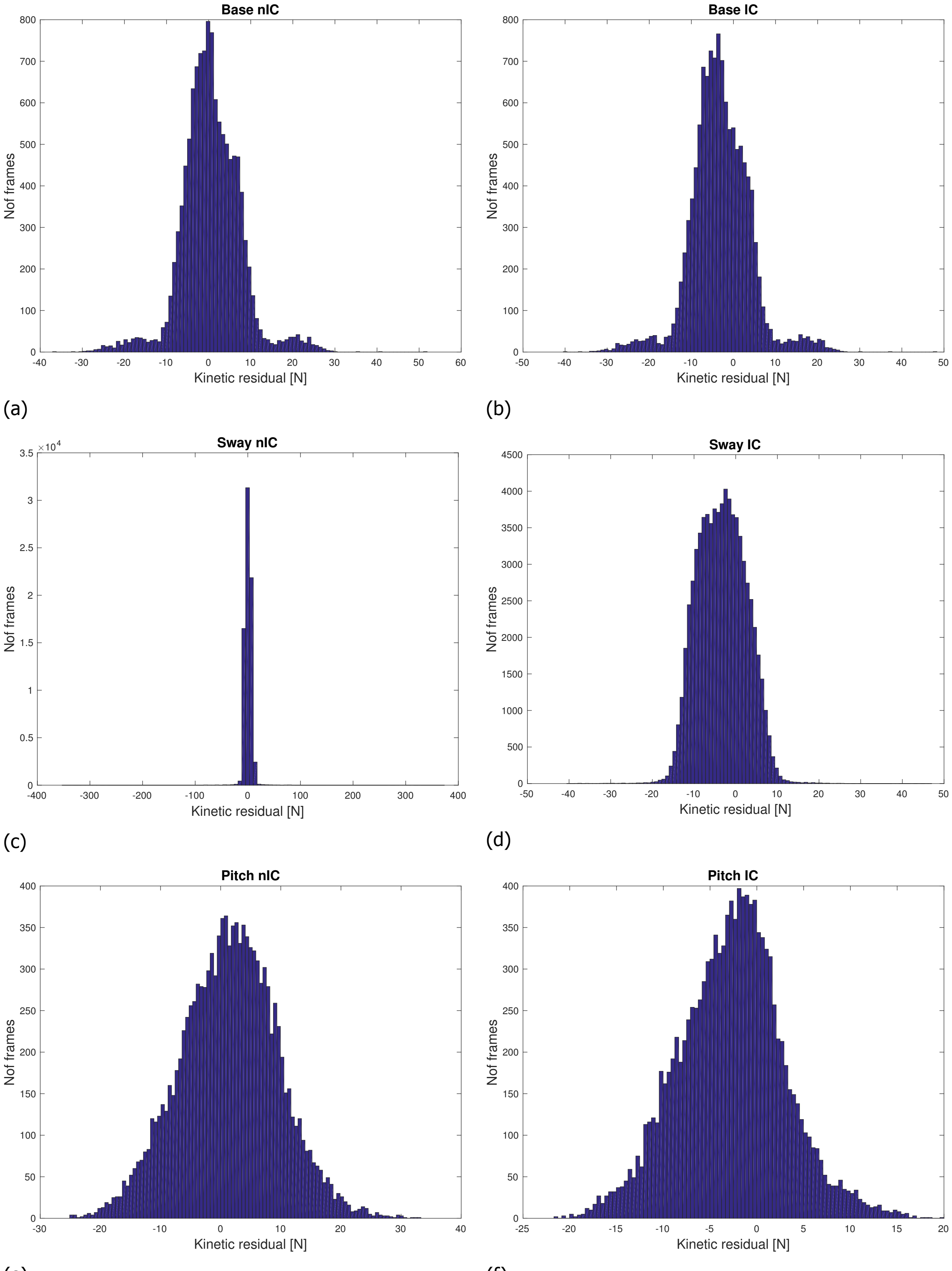

(a) (b)

(c) (d)

(e) (f)

Figure F.19: Raw data of the kinetic residuals of one subject for moment Z. The number of frames (nof frames) is shown for all conditions with IC (IC) and without IC (nIC).

G

Consent Form

Consent Form

The effect of inertia compensation during treadmill perturbations

Please tick the appropriate boxes	**Yes**	**No**
Taking part in the study		
I have read and understood the study information dated 16/10/18 or it has been read to me. I have been able to ask questions about the study and my questions have been answered to my satisfaction.	☐	☐
I consent voluntarily to be a participant in this study and understand that I can refuse to answer questions and I can withdraw from the study at any time, without having to give a reason.	☐	☐
I understand that taking part in the study involves walking on a treadmill while being perturbed, body measurements (forces, movement) and a questionnaire with general information in which I will provide my gender and age.	☐	☐
Risks associated with participating in the study		
I understand that taking part in the study involves the following risks: During the experiment you will be exposed to perturbations which could disturb your balance but cannot lead to a fall to the floor as you are wearing a safety harness.	☐	☐
Use of the information in the study		
I understand that information I provide will be used for statistical analysis for a master thesis and a possible publication directly related to this research.	☐	☐
I understand that personal information collected about me that can identify me, such as [e.g. my name or where I live], will not be shared beyond the study team.	☐	☐
Future use and reuse of the information by others		
I give permission for research data, so the body measurements, that I provide to be archived in the data repository of the Prof. dr. F.T.H. van der Helm at the TU Delft. The data will be anonymized archived so it can be used for future research and learning.	☐	☐

Signatures

________________________ ________________________ _________

Name of participant Signature Date

I have accurately read out the information sheet to the potential participant and, to the best of my ability, ensured that the participant understands to what they are freely consenting.

___________________________ ____________________ _________

Researcher name Signature Date

Study contact details for further information: Arianne van de Loosdrecht, +31623339358, A.E.P.vandeloosdrecht@student.tudelft.nl

H

Participant Information Sheet

Participant information sheet

The effect of inertia compensation during treadmill perturbations

This document provides more information on the purpose, procedures, risks and possible discomforts of this experiment. Please take time to read the following information carefully before agreeing to participate in this study. If anything you read is unclear or if you would like more information please ask for this.

Purpose of the research

The purpose of this research is to look at the effect of a model which is used in balance training. To train balance while walking on a treadmill, perturbations (sudden movements of the treadmill) can be given. The treadmill is also able to measure the forces that people apply on it. To calculate these forces more accurately, a model is used which will be tested in this study. This can help improve training and analysis of (impaired) balance. The results of this experiment will be statistically analyzed and published in a master thesis and might be used for a publication. The experiment is part of a project with cooperation of Motekforce Link and the TU Delft.

Inclusion criteria

All young adults (18-35 years old) without any neurological or orthopedic conditions that influence balance or walking can participate.

The experiment setup

The experiment will be done on a treadmill with a virtual reality environment called the GRAIL (Motekforce Link). A harness attached to the ceiling is provided for safety purposes. You will receive 26 markers that will be placed on different joints. Ten infrared cameras are placed around the treadmill which can capture the position of the markers and follow their trajectory.

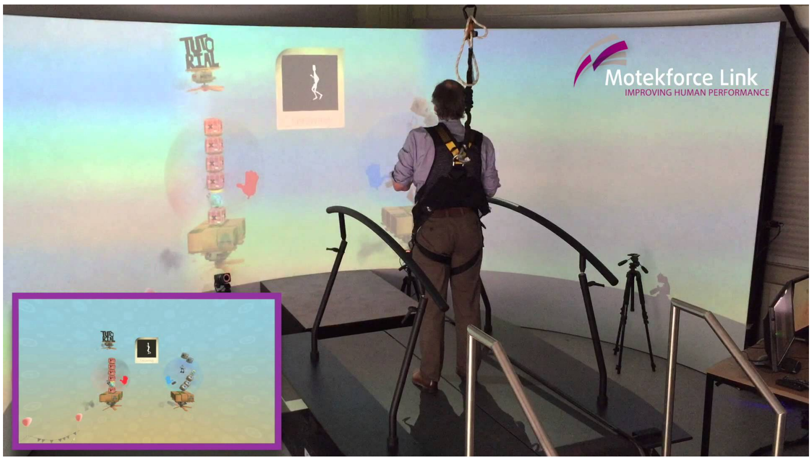

Figure 1. Treadmill, virtual reality environment and safety harness

Procedure

After reading these instructions and filling in the informed consent you will be asked to put on the appropriate clothing. A safety harness and 26 markers will be attached. Those markers will be placed on your trunk, legs and feet and will stick to your clothing or skin with some tape. These markers allow the cameras to capture your movement.

You are then ready to start walking on the GRAIL. First you will have six minutes to get familiar with walking on the treadmill. After this the real experiment will start. The experiment consists of three consecutive trials in which perturbations will take place. The perturbations include a part with sudden sideways movements of the treadmill which affect your balance and a part that includes up- and downhill walking. This will all be done at an average walking speed (4.7km/h).

During the whole experiment you should try to walk like you would in normal life. After a perturbation, try to start walking like you normally would as quickly as possible.

All together you will be walking on the treadmill for 20-25 minutes. The entire experiment will take about 45 minutes.

Preparation

To obtain accurate results it is important that all markers can be seen by the cameras and are not covered by clothing. Furthermore, any reflective parts on clothing, shoes or jewelry will give bad results as this can be seen as a marker. To ensure this, please take some (sports) clothing that tightly fits your body and does not have any reflective parts. If this is a problem, there are shoes and some clothing at the facility as well.

Benefits and risks of participating

Risks: you are asked to walk on a treadmill for 20-25 minutes at an average walking speed. This can cause some fatigue.
Benefits: there are no benefits or compensation for participating in this experiment.

Discomfort and withdrawal from the study

If you feel uncomfortable in any way or for any reason, you can always ask the researcher to stop the treadmill. You have the right to withdraw from the experiment at any time without mentioning any reason or consequences.

Confidentiality and privacy

This experiment will collect movement and force data from the experiment setup. Age, body weight, gender and body length will be used to calculate the mean data for the general subject from which the results will be derived. All collected data will be:

- Anonymized, subjects are referred to by only a subject number (e.g. sub01) of which the key will be held by prof. dr. F.T.H. van der Helm.
- Kept confidential.
- Used for a master thesis and a possible publication.
- After this research, data will be archived in the data repository of the Prof. dr. F.T.H. van der Helm at the TU Delft and can be used for future research and learning.

Questions and complaints

If you have any questions or complaints regarding the experiment or research you can contact Arianne van de Loosdrecht, her contact details are listed below.

Contact details

Researcher:	**Supervisor TU Delft:**	**Supervisor Motekforce Link:**
MSc. Student Arianne van de Loosdrecht	Prof. Dr. Frans C.T. van der Helm	Selma Papegaaij PhD
A.E.P.vandeLoosdrecht@student.tudelft.nl	F.C.T.vanderHelm@tudelft.nl	selma.papegaaij@motekforcelink.com
+31 6 23339358		

TU Delft

Motek
a DIH brand

Bibliography

[1] L. H. Sloot, H. Houdijk, and J. Harlaar, *A comprehensive protocol to test instrumented treadmills,* Medical Engineering and Physics **37**, 610 (2015).

[2] P. Merriaux, Y. Dupuis, R. Boutteau, P. Vasseur, and X. Savatier, *A Study of Vicon System Positioning Performance,* Sensors **17**, 1591 (2017).

[3] L. Aarts, S. Papegaaij, F. Steenbrink, and P. Martens, *QUALITY OF TREADMILL EMBEDDED FORCE PLATES FOR GAIT ANALYSIS,* (2018).

[4] G. Paolini, U. Della Croce, P. O. Riley, F. K. Newton, and D. C. Kerrigan, *Testing of a tri-instrumented-treadmill unit for kinetic analysis of locomotion tasks in static and dynamic loading conditions,* Medical Engineering and Physics **29**, 404 (2007).

[5] E. Fortune, J. Crenshaw, V. Lugade, and K. R. Kaufman, *Dynamic assessment of center of pressure measurements from an instrumented AMTI treadmill with controlled precision,* Medical Engineering and Physics **42**, 99 (2017).

[6] F. Dierick, M. Penta, D. Renaut, and C. Detrembleur, *A force measuring treadmill in clinical gait analysis,* Gait & posture **20**, 299 (2004).

[7] *Force plate nodes - Nexus 2.5 Documentation,* .

[8] S. R. Goldberg, T. M. Kepple, and S. J. Stanhope, *In Situ Calibration and Motion Capture Transformation Optimization Improve Instrumented Treadmill Measurements,* Journal of Applied Biomechanics **25**, 401 (2009).

[9] A. J. van den Bogert, T. Geijtenbeek, O. Even-Zohar, F. Steenbrink, and E. C. Hardin, *A real-time system for biomechanical analysis of human movement and muscle function,* Medical & Biological Engineering & Computing **51**, 1069 (2013).

[10] P. de Leva, *Adjustments to Zatsiorsky-Seluyanov's segment inertia parameters,* Journal of Biomechanics **29**, 1223 (1996).

[11] J. A. Reinbolt, A. Seth, and S. L. Delp, *Simulation of human movement: applications using OpenSim,* Procedia IUTAM **2**, 186 (2011).

[12] D. G. Lloyd and T. F. Besier, *An EMG-driven musculoskeletal model to estimate muscle forces and knee joint moments in vivo,* Journal of Biomechanics **36**, 765 (2003).

[13] A. D. Kuo, *A least squares estimation approach to improving the precision of inverse dy-namics computations*, Tech. Rep. (1995).

[14] S. L. Delp, F. C. Anderson, A. S. Arnold, P. Loan, A. Habib, C. T. John, E. Guendelman, and D. G. Thelen, *OpenSim: Open-source software to create and analyze dynamic simulations of movement,* IEEE Transactions on Biomedical Engineering **54**, 1940 (2007), arXiv:15334406 .

[15] I. Markovsky and S. Van Huffel, *Overview of total least-squares methods,* Signal processing **87**, 2283 (2007).

[16] I. Petráš and D. Bednárová, *Total Least Squares Approach to Modeling: A Matlab Toolbox,* Acta Montanistica Slovaca Ročník **15**, 158 (2010).

[17] S. K. Hnat, B. J. van Basten, and A. J. van den Bogert, *Compensation for inertial and gravity effects in a moving force platform,* Journal of Biomechanics **75**, 96 (2018).

[18] S. K. Hnat and A. J. van den Bogert, *Inertial compensation for belt acceleration in an instrumented treadmill,* Journal of Biomechanics **47**, 3758 (2014).

[19] A. J. van den Bogert, *PRACTICAL GUIDE TO DATA SMOOTHING AND FILTERING*, Tech. Rep. (1996).

[20] H. Woltring, *GCVSPL software package [Memorandum],* .

[21] R. W. BOHANNON, *Comfortable and maximum walking speed of adults aged 20—79 years: reference values and determinants,* Age and Ageing **26**, 15 (1997).

[22] J. Zeni, J. Richards, and J. Higginson, *Two simple methods for determining gait events during treadmill and overground walking using kinematic data,* Gait & Posture **27**, 710 (2008).